Aus der Neurologischen Klinik und Poliklinik der
Universität München

Direktorin: Prof. Dr. med. Marianne Dieterich

Torsional Control of Eye-Head Saccades

Dissertation
zum Erwerb des Doktorgrades der Medizin
an der Medizinischen Fakultät der
Ludwig-Maximilians-Universität zu München

vorgelegt von
Bernhard M. Blum
aus Landshut

2013

Mit Genehmigung der Medizinischen Fakultät
der Universität München

Berichterstatter:	Prof. Dr. med. Ulrich Büttner
Mitberichterstatter:	Priv. Doz. Dr. med. Eike Krause
	Prof. Dr. med. Oliver Ehrt
Mitbetreuung durch den promovierten Mitarbeiter:	Dr. Ing. Thomas Eggert
Dekan:	Prof. Dr. med. Dr. h.c. Maximilian Reiser, FACR, FRCR
Tag der mündlichen Prüfung:	07.11.2013

Contents

1. Introduction

This thesis examines and discusses how the central nervous system controls the three-dimensional motor behavior of the eyes and the head in visual orienting. The question is addressed functionally through neurophysiological experiments by analyzing data on the measured physical responses to various stimuli and identifying rules that relate quantitative stimulus and response characteristics. The focus of this investigation is on torsional control of combined eye-head gaze shifts and how these observations influence formal descriptions of the related parts of the nervous system.

Controlling the three-dimensional rotatory movements gives rise to particular challenges for neural control. By descriptive, analytical and modeling approaches, neuroscience and sensorimotor research are only about to begin to understand the control of combined three-dimensional eye-head gaze shifts. Until recently investigations largely focused on behavioral constraints that reduce the torsional freedom of the eye and the head during visual fixation (see Background section 2.3.2). To date, it remains unclear whether torsional constraints of an eye-head gaze position are influenced by the direction of the saccade preceding this fixation. Unveiling these constraints is essential in understanding what torsional control of eye-head saccades is trying to optimize under natural viewing conditions. The primary objective of this study is to perform this analysis for eye and head movements simultaneously during head-free gaze shifts. Results will be interpreted from an eye-head control point of view.

As a secondary objective control data from healthy adults are collected and presented in order to improve identification and quantification of gaze movement disorders in clinical context. Clinical applications of three-dimensional approaches to the oculomo-

tor system are highly researched for the last two decades [Fetter and Haslwanter, 1999, Henn and Straumann, 1999]. Neurophysiological experiments in patients are becoming a common diagnostic tool in this area. Indications include loss of vestibular function [Aw et al., 1999], strabism and eye muscle palsies [Bergamin et al., 2001], peripheral and central unilateral fourth and sixth nerve palsies [Wong et al., 2002a, Wong et al., 2002b] as well as midbrain and cerebellar lesions [Buettner et al., 2002, Glasauer et al., 2003].Recent examples of studies on vertical-torsional saccade generation are from a research group at the Department of Neurology, University of Munich, that examined patients with unilateral midbrain lesions [Kremmyda et al., 2007, Kremmyda et al., 2011]. Therefore for this study the gaze movement paradigms were designed to provide control data that are comparable to the last-mentioned patient experiments.

2. Background

For the course of this thesis *gaze* is defined as the orientation of the eye-in-space. *Eye (position)* on the other hand refers to the orientation of the eye-in-head.

2.1. An Eye-Head Gaze on Bernstein's Problem

Every single gaze shift poses the problem of selecting a combined three-dimensional eye and head motion from infinitely many alternative possibilities. Consider the simple task of reading a text. To read these lines, you have to shift your gaze from left to right in short, fast, angular displacements called *saccades*. These saccades can be accomplished by keeping your head still and only moving your eyes inside the head. Alternatively, depending on your viewing distance to the manuscript or to the computer screen (and other parameters), your head can contribute any amount to the gaze displacement. From the combination of three-dimensional eye and head (and even torso and foot) movements arise infinite alternatives to perform a single gaze shift [Guitton et al., 2003].

Given an infinite number of ways to perform a task, does the brain choose the same way every time, and if so, what rule does it follow? Almost half a century ago the Russian physiologist Nikolai Aleksandrovich Bernstein (1896 - 1966) called this the *degrees of freedom problem* [Bernstein, 1967, Turvey, 1990, Crawford and Vilis, 1995]. Any of the limited number of ways in which a body unit like the head or eye may move is called a degree of freedom. In three-dimensional space bodies can have a maximum of six degrees of freedom. These are two ways of motion - translation and rotation - in each of the three body planes: sagittal, frontal, and axial. When focusing only on rotatory motion, any

combined movement of head and eye has six (rotatory) degrees of freedom: three each for the two body units. The resulting gaze shift on the other hand has only two degrees of freedom. It is completely defined by two relative target coordinates that specify the horizontal and vertical angular displacements from current gaze position to the following word, line or paragraph. This system is *under-defined* in that the *two* target parameters of the gaze shift (*dependent* variables) depend on *six* rotation parameters of head and eye (*independent* variables). According to Bernstein, the brain tries to solve this excess or *redundancy* of degrees of freedom by using the smallest possible number of control parameters. He defined *coordination* as a problem of reducing the number of independent variables in order to master a particular movement [Bernstein, 1967].

Besides being a source of complex computational problems, redundant degrees of freedom are also the basis of the versatility of biological systems - that is, the beings' ability to perform different tasks in a wide range of environmental conditions [Bizzi et al., 1991]. Thus unveiling the constraints implemented to reduce redundant control parameters provides insight into what the brain is trying to optimize. In this context, the following question is equally relevant in sensorimotor research, computational neuroscience and robotics:

What are the constraints of three-dimensional head and eye movements in combined gaze shifts?

2.2. Donders' Law Solves Torsional Redundancy

It is tempting to think that a trivial solution to Bernstein's problem would be to simply keep the head still and visually explore the environment by mere eye movements. While this would render us pretty stiff-necked, it also does not get to the crux of the matter. Even under conditions that prevent movements of the head, the human oculomotor plant itself, consisting of muscles, connective tissue and orbital mechanical properties, is kinematically redundant. That is, it has more than the two degrees of freedom required for the description of a gaze task. This kinematic redundancy results from the eye's capacity of rotating about three linearly independent axes that pass through the center of the rotation of the globe (see Figure 2.1) [Fick, 1854, Nagel, 1868, Collewijn et al., 1985, Misslisch et al., 1994, Hess and Angelaki, 1997]:

1. the anteroposterior or sagittal x-axis, to generate torsional eye rotations (excyclotorsion and incyclotorsion),

2. the horizontal y-axis to generate vertical eye rotations (elevation and depression), and

3. the vertical z-axis to generate horizontal eye rotations (abduction and adduction).

Figure 2.2 illustrates torsional redundancy of the eye. The direction of the gaze, as the controlled entity, only has a horizontal and a vertical degree of freedom. Ocular torsion remains unspecified by gaze coordinates. Thus, in Figure 2.2 the eye could assume an infinite number of torsional orientations and still gaze straight ahead. With regard to the eye rotations, the first part of Bernstein's problem can now be rephrased: If there is an infinite number of possible torsional positions for each gaze direction, does the eye adopt one or multiple torsional position(s) for a particular gaze direction?

One solution of kinematic redundancy is a constraint described by the Dutch ophthalmologist Franciscus Cornelis Donders (1818 - 1889). It was found for steady fixation of distant targets with the head fixed and upright: The so-called *Donders' law* states that for any unique gaze direction, regardless of how it was reached by the eye, the brain always

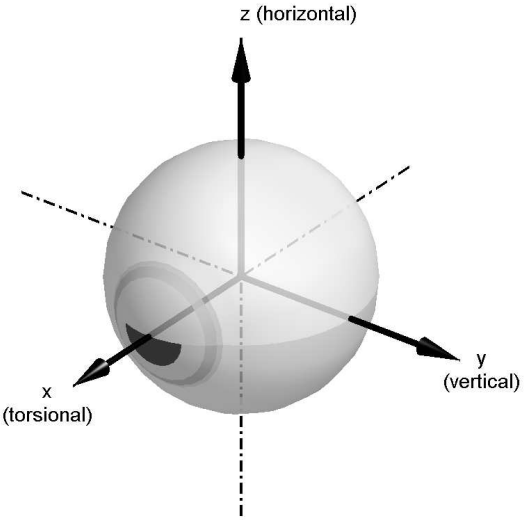

Figure 2.1.: Eye globe and the three axes of eye rotation. The eye rotates torsionally about the x-axis (*roll*), vertically about the y-axis (*pitch*) and horizontally about the z-axis (*yaw*). (Adapted from [von Noorden and Campos, 2002])

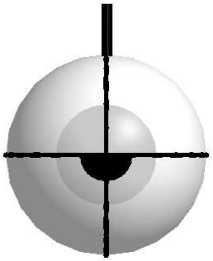

(a) 12 o'clock

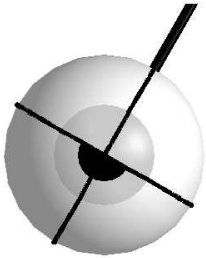

(b) 1 o'clock

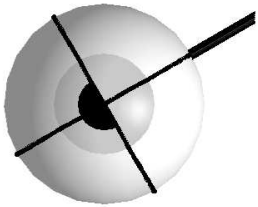

(c) 2 o'clock

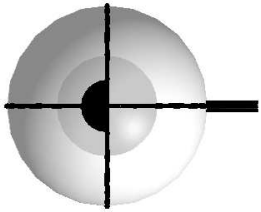

(d) 3 o'clock

Figure 2.2.: The eye at gaze straight ahead but with four different torsional orientations. The superior pole of the eye schematics in subfigures 2.2a-2.2d is marked by the thick black line sticking out of the globe. There are infinitely many different torsional orientations that the eye can adopt without changing the direction of gaze: 12 o'clock (2.2a), 1 o'clock (2.2b), 2 o'clock (2.2c), 3 o'clock (2.2d), and so on. (Adapted from [Wong, 2004])

selects the same eye orientation in three-dimensional space [Donders, 1848]. All other eye positions consistent with the horizontal and vertical components of that respective two-dimensional gaze direction, but different in torsional orientation would violate the law. Therefore, the first part of Bernstein's problem can be answered: Given an infinite number of torsional eye rotations to perform a head-fixed gaze task, the brain *does* choose the same position every time. However, a *qualitative* constraint like Donders' law can not answer the second part of the degrees of freedom problem: What rule does the brain follow? Or asked in terms of three-dimensional eye-head coordination:

> What is the torsional angle that every horizontal-vertical eye and head position is constrained to in three-dimensional space?

2.3. The Shape of Donders' Surface

2.3.1. With the Head Restrained

The question about a *quantitative* description of the eye movement constraint implied by Donders' law was first answered theoretically by the German mathematician Johannes Benedict Listing (1808 - 1882). He put Donders' law as follows: For steady fixations of distant targets with the head fixed and upright, the brain restricts the possible set of all three-dimensional eye positions to a two-dimensional subspace by constraining torsional deviations. If this subspace was continuous from one gaze direction to the next, it would form a three-dimensional surface. This way, to quantitatively determine the torsional angle of each gaze position, one only has to know the shape of this surface.

His result, known as *Listing's law*, is most simply described by expressing eye positions in terms of the axes of their rotational displacements from a single reference position. In doing so, *Euler's theorem* applies: it states that for every two orientations of an object, the object can always move from one to the other by a *single* rotation about *one* fixed axis [Euler, 1775]. Apparently, based on pure geometrical aesthetics, Listing stated that all those rotation axes, characterizing three-dimensional eye positions, lie on a flat plane - now called *Listing's plane* - fixed in the head [Westheimer, 1957]. Note that like Donders' law, Listing's law was equally formulated for steady fixations of distant targets with the head fixed and upright. The German physician and physicist Hermann Ludwig Ferdinand von Helmholtz (1821 - 1894) later confirmed this result experimentally by observing the systematic tilt of afterimages in various gaze directions [Helmholtz, 1863, Helmholtz, 1867]. Evidence based on eye movement recordings with the more precise magnetic search coil method can be found [Ferman et al., 1987, Tweed and Vilis, 1990, Tweed et al., 1994, DeSouza and Vilis, 1997].

In Figure 2.3 Listing's plane is represented by the gray plane and the orientation of the eye at the center would be defined as reference position. The nine eccentric globes outlined with black contours visualize admissible eye orientations, because they can be reached from

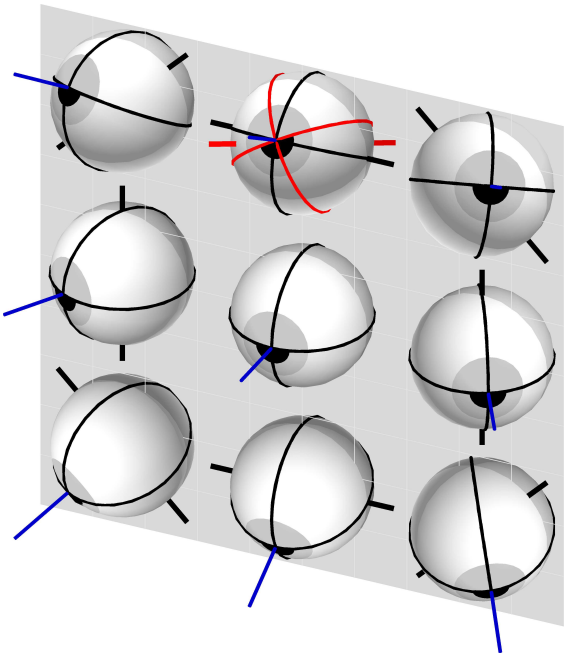

Figure 2.3.: Donders' law *qualitatively* constrains the orientation of rotation axes characterizing three-dimensional eye positions in relation to a reference position (central globe) to a two-dimensional surface of unknown shape. Listing's law then - for head-fixed gaze shifts - *quantitatively* defines the shape of Donders' surface as a flat plane (gray) secured in the head. The nine eccentric globes outlined with black contours visualize admissible eye orientations, because they can be reached from the central reference position by rotating about the axes (black lines) in Listing's plane. In the top center position a second globe (red contours) with identical line of sight (blue lines) but different torsional orientation is shown. Donders' law however only permits one torsional orientation for every gaze direction and Listing's law defines its angle (black axis). (Adapted from [Tweed and Vilis, 1990])

reference position by rotating about the axes (black lines) in Listing's plane. The position drawn with a red contour at the top center violates Listing's law, since the rotation to that orientation from reference position has its axis (red line) tilted out of Listing's plane. More importantly, Figure 2.3 depicts Listing's law as a quantitative implementation of Donders' law: For any direction of gaze, there is only one orientation assumed by the eye, and this orientation does not depend on the path taken to that gaze direction. For example, the two eye positions sketched in black and red at the top center both correspond to the same upward gaze direction as their blue gaze lines coincide, but Donders' law permits only one torsional orientation and its angle is defined by Listing's law (globe with black outline). Furthermore, Figure 2.3 illustrates how according to Euler's theorem any other position can be reached from the central globe by a single rotation about one fixed axis.

2.3.2. When the Head Contributes

In contrast to the artificial head-restrained condition of the aforementioned kinematic constraints, most natural orienting gaze shifts are accomplished by coordinated eye *and* head movements [Bizzi et al., 1971, Klier et al., 2001]. When gaze shifts are made under conditions that permit movements of the head, a number of issues arise.

- Do the constraints that define head-restrained saccades remain unaltered when the head is free to move?
- If not, what are the defining constraints of head-unrestrained gaze shifts?
- Are the controls of head and eye movements tightly linked in gaze shifts or are they independent?

Both for their importance in understanding the neurophysiology of head-unrestrained visual orienting and as a possible general model for coordination and control, such questions have been studied with increasing frequency during the last two decades. Early studies proposed an analogue of Listing's law for the head [Tweed and Vilis, 1992] and even for gaze and arm movements [Straumann et al., 1991]. By increasing the amplitudes of recorded eye

and head gaze shifts, Glenn and Vilis later noted that when using space-fixed instead of head-fixed coordinates, the axes of eye rotation do not lie on a plane. That is, gaze (eye-in-space) does not obey Listing's law. Instead, they found that three-dimensional gaze positions are constrained to a twisted surface. Therefore, gaze follows Donders' law but not in form of a (Listing's) plane [Glenn and Vilis, 1992]. Misslisch, Tweed and Vilis amended that the brain probably does not compute eye orientations based on the desired gaze direction alone, but also considers head orientation. That is, the eye position constraints in space described by Glenn and Vilis are simply a consequence of neural control of the head position and of the eye rotations relative to the head [Misslisch et al., 1998]. This finding was later confirmed by measurements in monkeys that led to the suggestion of quasi-independent three-dimensional eye- and head-control systems [Crawford et al., 1999]. In an attempt to further specify the reference frames of combined eye-head gaze shifts, Radau, Tweed and Vilis had standing subjects perform gaze shifts to an oversized target array. They found, that head orientations are calculated in a chest rather than a spatial frame of reference [Radau et al., 1994]. During repetitive head movements, the head violates Donders' law [Tweed and Vilis, 1992] analogous to the eyes that deviate from Listing's law during certain types of eye movements [Fetter et al., 1994]. In an interesting experiment with subjects wearing pinhole goggles, Ceylan, Henriques, Tweed and Crawford confirmed the task-dependence of eye and head movement constraints [Ceylan et al., 2000]. Tweed, Glenn and Vilis found that systematic departures from Donders' law also happen *during* combined eye and head gaze saccades as opposed to validity of the law *between* saccades [Tweed et al., 1995].

To date, it remains unclear whether the direction of the saccade preceding a fixation influences torsional constraints of gaze orientations and whether the neural controllers of the eyes and the head are independent in humans. The primary objective of this thesis is to perform this analysis for eye and head movements simultaneously during head-unrestrained gaze shifts in human subjects.

3. Methods

This chapter outlines the features of the conducted experiments and gives a description of the materials that were used. In all experiments, human subjects were stimulated visually and their eye-head gaze shifts were recorded with magnetic search coils for later offline analysis.

3.1. Subjects

Data of seven healthy adult subjects, without any known head or eye movement disorders or neurological pathologies, are presented (see Table 3.1). The subjects for this study were recruited from the research campus and by word-of-mouth. None of the subjects used spectacle correction during the experiments and visual acuity of all subjects was adequate to fixate the presented visual targets properly. Spectacle corrections induce magnification factors that change the direction of the line of sight and would hereby alter the resulting rotatory position of the eye (see Background section 2.3). Even though a calibration procedure can be executed to correct for this effect [Collewijn et al., 1983], this additional complication can be avoided by using emmetropic subjects. All subjects signed a paper of informed consent before the recordings (see Appendix section C). The experimental protocols adhered to the Declaration of Helsinki for research involving human subjects [World Medical Organization, 2004] and were approved by the local ethical committee.

ID	Gender	Age
DG	m	32
CC	f	28
OK	f	26
BD	m	28
BK	m	26
BB	m	24
PH	m	26

Table 3.1.: Overview of age and gender of the seven subjects, five male (m) and two female (f). Mean subject age is 27 years (SD = 2.5).

3.2. Recording Eye and Head Rotation

Rotations of both the left eye and the head about all three principal space axes (torsional/roll/x-axis, horizontal/pitch/y-axis, vertical/yaw/z-axis; see Background Figure 2.1) were simultaneously recorded with dual magnetic search coils while the subjects performed head-free gaze shifts. The magnetic search coil system measures the voltages in coils induced by three rapidly oscillating magnetic fields that are aligned with the principal space axes. This method of measuring eye rotation has considerable merit in that it has a large dynamic range, is virtually linear for angles up to 30 deg from primary eye position and does not limit the field of view [Robinson, 1963, Collewijn et al., 1975, Judge et al., 1980]. It is also less affected by blinks than other methods like video-oculography or infrared reflection devices as it continues to register data when the eye is closed. Due to its large signal to noise ratio and reliability, the search coil technique has been the generally accepted reference standard for eye rotation recordings for over 30 years [Henn and Straumann, 1999, Eggert, 2007].

3.2.1. Dual Magnetic Search Coils

To see why not one, but two nonparallel search coils are needed to record three-dimensional rotations, it is necessary to understand what the signal from a magnetic search coil represents. In the original paper on the method, Robinson showed that the signal Y from a coil in an alternating horizontal magnetic field is:

$$Y = G_\gamma \sin\theta \qquad \text{(Equation 3.1)}$$

where G_γ is a constant gain which depends on the coil and the field, and θ is the angle between the effective plane of the coil and the direction of the field [Robinson, 1963, Tweed et al., 1990]. In Figure 3.1, a search coil is seen edge-on from above and our line of sight is perpendicular to the direction of a horizontally oscillating magnetic field. Considering a vector c orthogonal to the effective plane of the search coil (see Figure 3.1), it is clear that any torsional rotation of the coil about an axis parallel to this normal vector does not change the angle θ between coil plane and field direction and therefore does not yield a

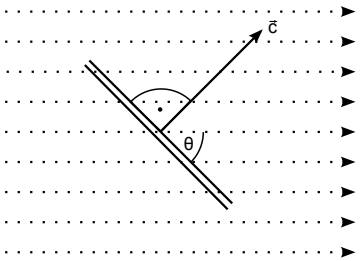

Figure 3.1.: The voltage induced in a search coil (double-line) by an oscillating magnetic field (dashed lines) is directly proportional to the sinus of the angle θ between the effective coil plane and the field direction (see Equation 3.1). In this figure, the coil is seen edge-on from above and our line of sight is perpendicular to the direction of a horizontal magnetic field. Notice that torsional rotations of the coil about a normal vector c, perpendicular to the coil plane, do not change the angle θ and therefore do not change the coil signal. (Adapted from [Tweed et al., 1990])

change of the coil signal Y (confirm in Equation 3.1). The same applies to magnetic fields oscillating in any other direction, that are not shown in Figure 3.1. So in order to register torsional together with horizontal and vertical rotations, a second coil whose effective plane must not be parallel to the plane of the first, directional coil and at least two nonparallel, oscillating magnetic fields are necessary.

Dual Scleral Search Coils

To gather three-dimensional rotation data of the eye a dual scleral search coil (manufactured by Skalar, Delft, The Netherlands) was used. Dual scleral search coils combine two coils that stand effectively orthogonal to one another in a single contact lens like device: a directional coil, that is oriented in the head-frontal plane, and a torsional coil, wound in a figure-eight-fashion, that has its effective area approximately in the sagittal plane (see Figure 3.2). The torsional sensitivity of the figure-eight coil becomes clear, when considering the image plane in Figure 3.2 as the subject's head-frontal plane. The figure-eight coil then projects as a single coil onto the sagittal plane, whereas the projections on the horizontal and frontal plane consist of two halves wound in opposite directions that cancel each other out. For a more comprehensive explanation of the functionality of the figure-eight coil see [Collewijn et al., 1985, Eggert, 2007]. Both coils are embedded in a medical-grade silicone annulus that is shaped to adhere to the limbus of the eye by slight suction (see Figure 3.3). For a detailed description of the silicone annulus see [Collewijn et al., 1975].

Scleral Search Coil Handling The scleral search coil was visually inspected for any defects or abnormalities before using it in the experiment. The coil was disinfected by immersion in a fresh 3 % hydrogen peroxide (H_20_2) solution for 20-30 minutes and rinsed in saline solution for at least 15 minutes before and after each trial.

Prior to the insertion of the suction ring, the subject's eye was briefly anesthetized externally by two subsequent drops of a topical ophthalmic anesthetic (oxybuprocaine 0.4 %). After 2-3 minutes the coil was inserted by hand and secured by applying the minimum amount of pressure necessary to prevent slippage of the coil. Anesthesia made

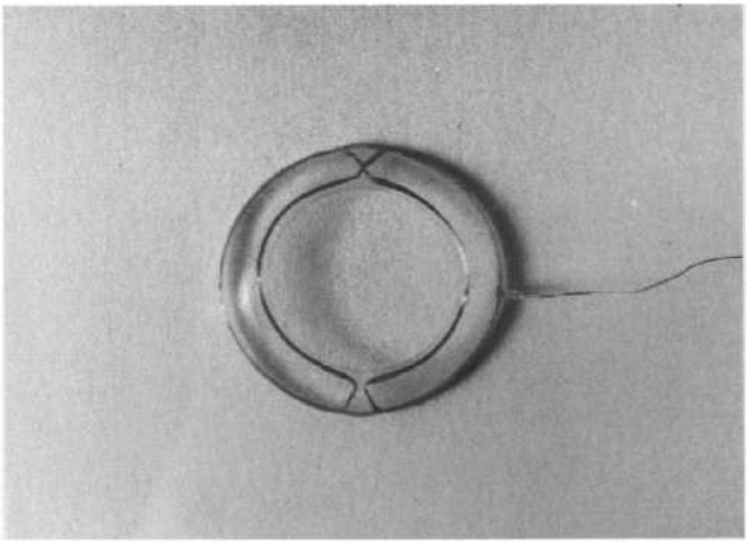

Figure 3.2.: Dual scleral search coils consist of a medical-grade silicone rubber suction ring with a suitable shape to adhere to the limbus of the eye. Embedded in the flexible ring are two induction coils wound of insulated copper wire: a directional coil used for measuring horizontal and vertical eye rotations wound in the frontal plane and an orthogonal coil which measures ocular torsion wound effectively in the sagittal plane (wires crossed in figure-eight-fashion).

the uncomfortable foreign body sensation (see [Irving et al., 2003]) bearable to all subjects for the duration of the recording (about 20 minutes). After insertion of the annulus, the exiting coil wire was fixed on the nasal bridge with medical tape in order to minimize contact with the eye lids. For a discussion of the influence of the exiting coil wire on ocular torsion, see [Bergamin et al., 2004]. The scleral search coil was removed after about 20 minutes or on request of either the subject or the clinician.

Dual Head Search Coils

Three-dimensional head rotations were measured using a dual head coil construction manufactured in our department: For each coil, four to five turns of insulated copper wire were wound around a plastic ring of approximately 2 cm in diameter. These coils were taped to a cubic support in the orientations of: 1) a directional coil oriented in head-frontal plane and 2) an orthogonal torsional coil oriented in head-sagittal plane. The assembled coil cube was fixed on an adjustable plastic ring to be firmly suited on the subject's head.

3.2.2. Magnetic Field System

The magnetic field system consisted of a cubic coil frame of welded aluminum with a side length of 140 cm that housed three pairs of Helmholtz coils (see Figure 3.4). These Helmholtz coil pairs are driven to produce three mutually orthogonal magnetic fields oscillating with three different frequencies of 55.5, 83.3, and 41.6 kHz and intensities of 0.088 Gauss (hardware by Remmel Labs, Ashland, Massachusetts, USA). Induced amplitude modulated signals were extracted synchronously from the search coils (modified Remmel system [Remmel, 1984]) resulting in three signal channels per coil (torsional, horizontal, vertical) and a total of twelve channels for the setup with two dual search coils (eye-directional/-torsional, head-directional/-torsional).

Search Coil Calibration

Immediately before each eye and head rotation recording, the magnetic search coil system was calibrated in a two-step procedure:

Free Calibration. In a first free calibration step, each dual search coil (eye, head) was rotated manually within the coil frame at the approximate site, where the subject's eye or head would be located during later recording. A large subset of all possible horizontal and vertical rotations was covered to determine the magnitude and relative orientation of the three magnetic fields and the gain of the directional coil. For a detailed description of this procedure see [Glasauer et al., 2003].

Fix Calibration. In a second fix calibration step, the offsets and the gain of the torsional coil, as well as the relative orientation of the coil on the eye or the head, were determined. The subject was first fitted with the previously free calibrated dual head search coil, which was firmly strapped to the head. The subject was seated upright in the magnetic field with the head in a position, which felt like the "natural zero position". Calibration data were recorded while the subject was repeatedly pointing his/her nose or the beam of a small head mounted laser at different target positions. The data set with the bigger range of head rotations was used for calibration of the head coil. The subject then was fitted with the likewise free calibrated dual scleral search coil and the head was immobilized by a firm chin rest. Again, calibration data were recorded, while the subject was repeatedly performing head-fixed gaze shifts to different target positions. The calibration did not depend on accurate fixation of these targets.

Test Space of the Magnetic Field System

The search coil recordings should be sensitive only to eye and head rotations, and unaffected by any translatory movements. To achieve this, the magnetic fields have to be homogeneous in strength and direction over a space including any possible head position. Ditterich and Eggert [Ditterich and Eggert, 2001] pointed out, that field inhomogeneities of the magnetic

search coil system stay below five percent inside a central cubic test space with an edge length of one-fifth of the field coils' edge length. In the described setup this resulted in a cubic test space of 28 cm edge length. Therefore, during recordings subjects were seated inside the field coil frame, so that the center of their interpupillary line coincided with the center of the frame (see Figure 3.4). A stationary wooden chair with a firm back support stabilized the subject's trunk and shoulders and helped to keep the subject's eyes and head in that central test space during calibration and signal recording (see Figure 3.4).

Data Sampling

Raw voltage data from the search coils were sampled digitally at 1 kHz with a *R*eal-time *EX*perimentation software system (*REX*, National Eye Institute, Bethesda, Maryland, USA) using a 12-bit analog to digital (AD) converter. The sampling computer was running the QNX real-time operating system (QNX, Ottawa, Ontario, Canada). These coil signal samples were stored on a local hard drive, uniformly spaced at one millisecond time intervals.

Figure 3.3.: Scleral search coil adhering to the limbus of the eye. The ocular side (concave) of the suction ring is slightly more curved than the eyeball. Capillary and suction forces hold the suction ring firmly in its place when the air and fluid between the eye and the suction ring is evacuated by slight pressure.

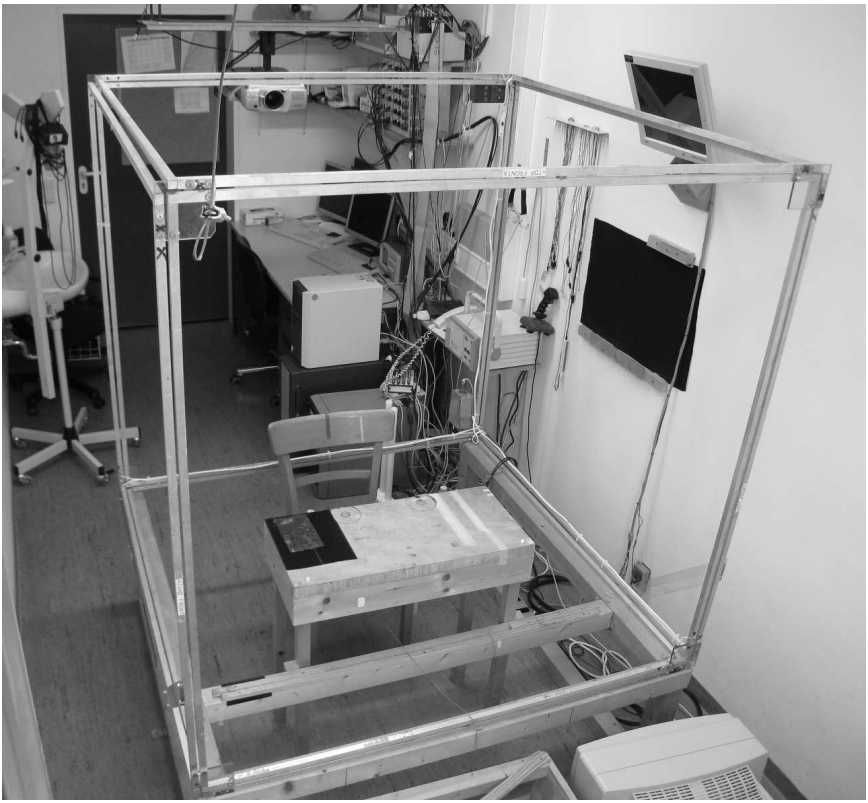

Figure 3.4.: Coil frame of the magnetic field system in the oculomotor laboratory in the Center for Sensorimotor Research at the Department of Neurology, Ludwig-Maximilians-University Munich (Germany). The four vertical faces of the cube (front-back and left-right) and the two horizontal faces (top-bottom) contain three pairs of Helmholtz coils. The coils have a side length of 140 cm and can be driven to produce three mutually orthogonal oscillating magnetic fields. At the center of the coil frame, a wooden chair with a firm back support is located. During recordings subjects were seated on this chair.

3.3. Visual Stimulation

Subjects made eye-head gaze shifts in response to visual stimuli provided by laser dots (0.1 degrees in diameter) projected on a screen 145 cm in front of them.

3.3.1. Stimulation Setup

Figure 3.5 shows the complete setup for generating the visual tasks and recording the subject's eye and head rotations. Visual stimuli were provided by a laser scanner system consisting of a diode laser and x-y mirror galvanometers for precise horizontal and vertical positioning of the laser beam (manufactured by General Scanning, Bedford, Massachusetts, USA). The projected laser dots measured 0.1 degrees in diameter on the screen so subjects had no problems fixating them considering a diameter of the fovea of about 2-3 degrees visual angle.

The projection screen was positioned at the maximum possible distance of 145 cm from the subject, given the constraints of laboratory space and configuration. Ideally, the visual targets should be at optical infinity. If this is not the case, any translations of eye and head will change the angular direction of the target and thereby the rotatory position of the eye (see Appendix section B). Also, the vergence angle between the subjects eyes changes when fixating different target positions on a flat screen that is not at optical infinity. Donders' law, however, is only defined for parallel lines of sight of both eyes, i.e. for visual targets at optical infinity, since the constraints of ocular torsion change during convergence in near vision [Allen and Carter, 1967, Van Rijn and Van den Berg, 1993, Bruno and van den Berg, 1997, Kapoula et al., 1999, Steffen et al., 2000]. Besides, during strong convergence the entire eye is temporally displaced within its orbit and the horizontal axis of ocular rotation is displaced forward within the globe contributing to small but systematic errors of recordings [Enright, 1980, Enright, 1984, Demer et al., 2003]. With the setup described the vergence angle was smaller than 2.5 degrees throughout all experiments (assuming an interpupillary distance of 6.5 cm).

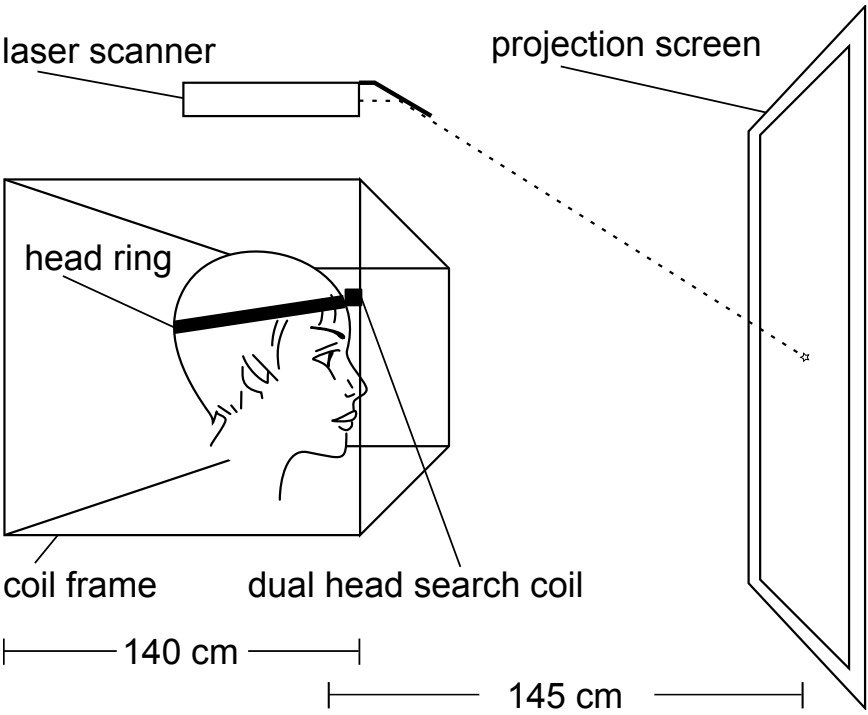

Figure 3.5.: Experimental setup for generating visual tasks and recording eye-head gaze shifts. Subjects were seated with their head in the center of the magnetic field coil frame (side length 140 cm). A laser scanner projected red dots (0.1 degree in diameter) on a screen at a distance of 145 cm. Eye and head rotations were recorded by dual magnetic search coils while subjects performed head-free gaze shifts to different target locations. All experiments were recorded in complete darkness except for the light of the point target.

3.3.2. Visual Target Array

The visual target array consisted of nine laser positions arranged in a square grid centered in front of the subject. This array is represented by the empty circles in Figure 3.6 and by the black dots in Figures 3.7a and 3.7b respectively. The central target was placed at the central gaze position (straight ahead), the four cardinal targets were positioned at 28 degrees eccentricity left, right, above and below it, and the four oblique targets were at 38.5 degrees eccentricity from the center. This array of visual targets was selected as large as possible under given laboratory premises to clearly distinguish between Listing's law and other forms of Donders' law which result in position ranges that mainly differ at the corners (see Background section 2.3.2).

3.3.3. Paradigms

To be comparable to each other, the two experiment paradigms only differed in the sequence of laser target steps between the fixed positions of the target array. All recordings were done in complete darkness except for the light of the point target. At any given time only one visual target was visible. A single trial consisted of a fixation followed by a target step and a subsequent fixation (see Figure 3.6). Individual trials were separated by an interval of complete darkness (laser target not visible). Subjects were instructed to foveate the laser targets by natural eye-head gaze shifts and to try and stabilize their line of sight on the respective target position during darkness in the interval time until the next trial started.

Star Paradigm

In the Star paradigm (Figure 3.7a), the laser target dot stepped to all target positions four times from the *same direction*. Thus, the laser target dot stepped to eight eccentric target locations always from the center. Target steps to the center had their single origin in the upper right corner. As shown in Figure 3.7a the trajectories of the laser dot form a star pattern.

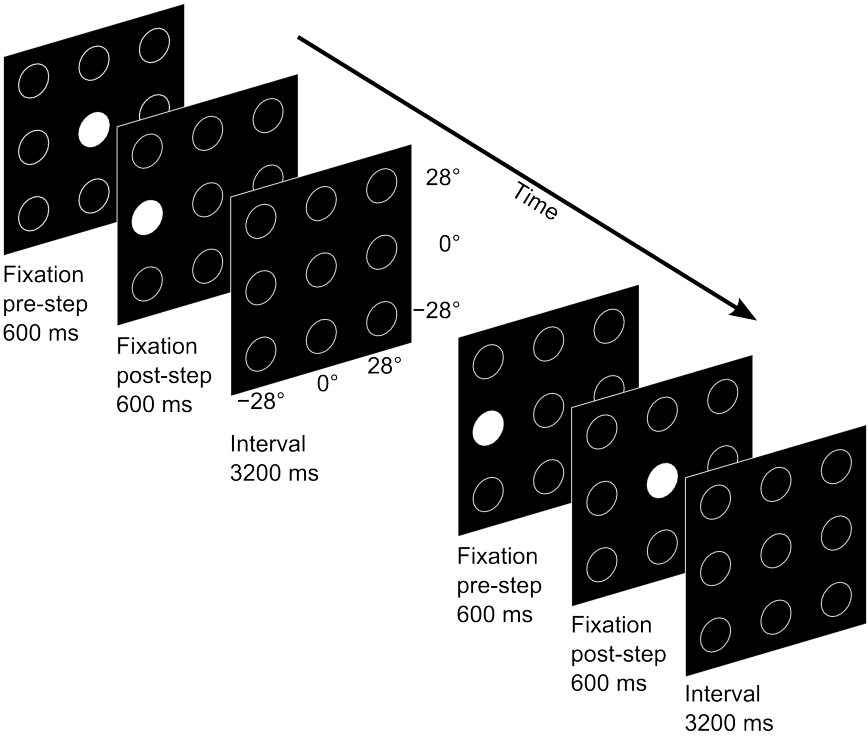

Figure 3.6.: Flow chart of the first two trials of the Star paradigm (see Subfigure 3.7a). Each trial began with fixation on one of the nine target positions. Then, the laser pseudo-randomly stepped to another fixation target. Subjects were requested to maintain the new gaze position during the interval until the next trial started at the location where the target was last visible. In the panels all positions of the laser target array are marked by empty circles. These marks are just shown for the purpose of this figure. Subjects could only see the single laser dot on an otherwise black screen.

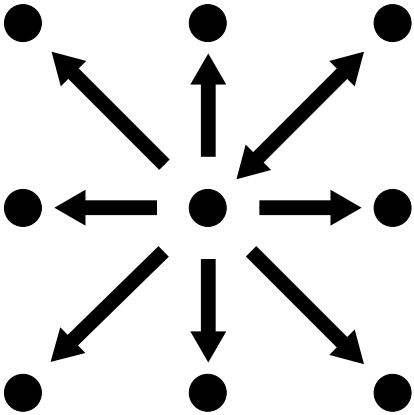

(a) Star Paradigm

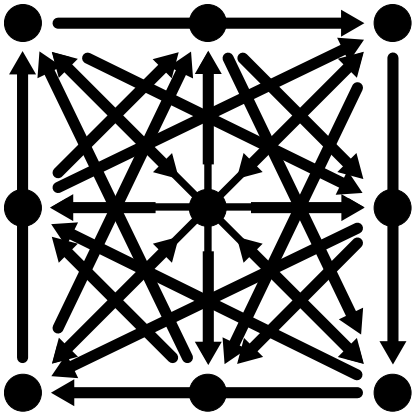

(b) Diamond Paradigm

Figure 3.7.: Visual Paradigms: The target array positions are marked by filled circles and the steps of the laser dot stimulus by arrows. In the Star paradigm (3.7a), the laser dot stepped four times to every target position from the *same initial position*. In the Diamond paradigm (3.7b), the laser dot stepped four times to each of the peripheral target positions from *different initial positions*.

Diamond Paradigm

In the Diamond paradigm the laser dot stepped to all target positions four times from *different directions*. For example eye-head gaze shifts to the upper right target position in Figure 3.7b were carried out once from each of the three target spots on the left (upper, middle, lower) and from the center location in pseudo-random order during the experiment.

3.4. Analysis

The recorded search coil signal samples were downloaded onto a standard PC and analyzed off-line using in-house software developed in MATLAB Version 7 (The MathWorks, Natick, Massachussets, USA) and a SQLite database.

3.4.1. Noise Filter

In the first step of processing, the calibrated raw data were smoothed with a digital low-pass filter having a cutoff frequency of 33 Hz in order to attenuate undesirable high frequency components (*noise*). A Gaussian filter was used for this task to maintain important saccade characteristics like steep signal edges.

3.4.2. Gaze, Head and Eye Quaternions

The filtered search coil signals were converted into gaze and head position quaternions using a method described by [Tweed et al., 1990]. Throughout this paper, the gaze and head quaternions are expressed in a right-handed coordinate system (see Appendix section A.1) aligned with the space-fixed magnetic fields of the Helmholtz coils. Then the position of the eye-in-head had to be computed from both the gaze quaternions (eye position in space) and the head quaternions (head position in space). In one dimension, this would be done by subtracting head position from gaze position. In three dimensions, this was done by dividing the gaze quaternion by the head quaternion as follows:

$$Eye = (Head)^{-1}Gaze \qquad \text{(Equation 3.2)}$$

This provides the quaternion for eye position in head coordinates. Note that for displaying purposes throughout this thesis, quaternion units were scaled by $360\frac{deg}{\pi}$ to approximate angular positions in degrees.

3.4.3. Angular Velocity and Fixations

Instantaneous angular velocity vectors were computed from position quaternions using a method described before (see [Crawford and Vilis, 1991]). These velocity vectors are aligned with the instantaneous axis of rotation and of length equal to the instantaneous angular speed of rotation. Like the quaternion vectors, the angular velocity vectors were expressed according to the right-hand rule, as described in Appendix section A.1.

A velocity threshold criterion [Salvucci and Goldberg, 2000] was then used to identify fixations. Therefore, the fixation range was defined as positions where the velocities (more correctly the one-dimensional magnitudes of the three-dimensional instantaneous velocities) of both gaze and head were below a threshold of 10 deg/s.

3.4.4. Second Order Surface Fits

In order to describe the torsional components of gaze, head or eye positions as a function of their respective horizontal and vertical positions, the quaternion data were fitted to a second-order surface by a previously described procedure [Glenn and Vilis, 1992, Radau et al., 1994, Tweed et al., 1990]. In short, a multiple linear regression is applied to the sampled quaternion data. The following formula provides the equation for a second-order fit with generic position quaternions (q):

$$q_1 = a_1 + a_2 q_2 + a_3 q_3 + a_4 (q_2)^2 + 2a_5 q_2 q_3 + a_6 (q_3)^2 \qquad \text{(Equation 3.3)}$$

This is the three-dimensional analogue to the equation of a one-dimensional line in two-dimensional space:

$$y = ax + b \qquad \text{(Equation 3.4)}$$

It represents a description of torsional position q_1 as a function (through coefficients a_1 to a_6) of various combinations of vertical (q_2) and horizontal position (q_3) up to the squared terms. During the fitting procedure the coefficients of this equation were selected to minimize the scatter of the data in torsional direction.

Once such a surface of best fit had been computed, the standard deviation (SD) of the torsional residuals of all fixations from this fit was computed using the method described previously (see [Tweed and Vilis, 1990]). This measure is also commonly called "torsional thickness" of the sampled position data.

3.4.5. Surface Fit Coefficients

Figure 3.8 gives an overview of the effect of the different fit coefficients a_1 to a_6 of a second-order surface. For the description of a planar so-called first-order surface only the first three terms of Equation 3.3 would be necessary. Second-order surfaces on the other hand can be parabolic or twisted. Therefore, the first six subfigures from 3.8b to 3.8g show planes, whereas the remaining subfigures from 3.8h to 3.8m show non-planar parabolic or twisted surfaces.

The offset of the fitted surface along the torsional axis is given by the a_1 term: Negative a_1 values indicate an overall tendency to keep the eye rotated counterclockwise (3.8b). Positive a_1 values are due to a general clockwise rotated eye position (3.8c). Coefficient a_2 determines the horizontal slope of the fitted surface: A subject with a negative a_2 value rotates the eye counterclockwise when looking down and rotates it clockwise, when looking up (3.8d). For a positive a_2 value it would be the other way round (3.8e). Correspondingly, coefficient a_3 results in a vertical slope of the fitted surface: Eyes that rotate counterclockwise when looking to the left and clockwise at gaze to the right show negative a_3 values (3.8f) and in the opposite case a_3 would be positive (3.8g).

Both coefficients a_4 and a_6 result in parabolic surfaces. Coefficient a_4 defines the horizontal curvatures of the fitted surface: Negative a_4 values describe that the eye rotates counterclockwise with every vertical gaze (up or down) and returns to zero torsion for purely horizontal gaze positions (3.8h). When vertical gaze induces clockwise eye torsion a_4 is positive (3.8i). Coefficient a_6 does the same for the vertical curvature of the fitted surface: A subject with a negative a_6 value rotates its eye counterclockwise for every horizontal (left or right) gaze deviation (3.8l). If the torsion is increasingly clockwise for

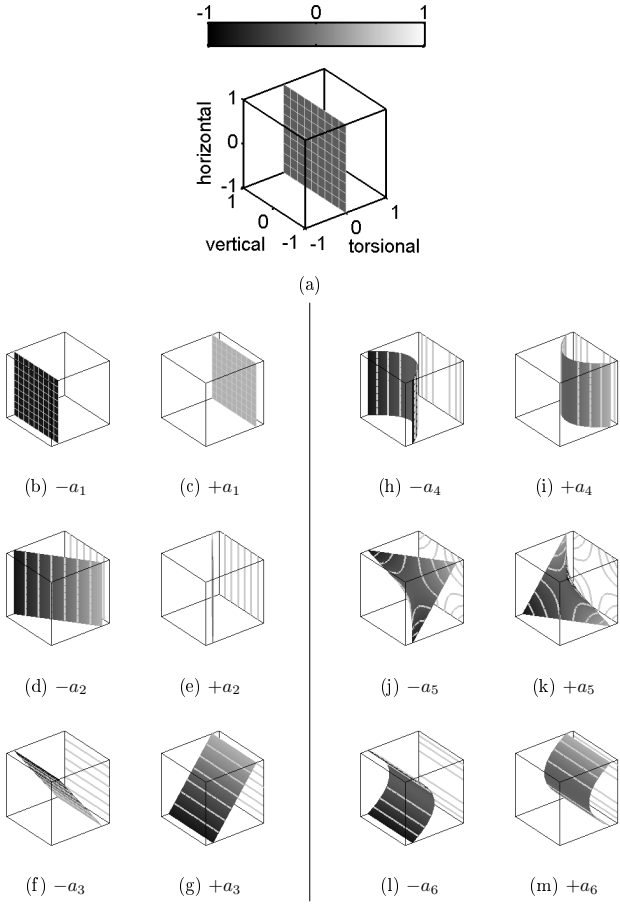

(a)

(b) $-a_1$ (c) $+a_1$ (h) $-a_4$ (i) $+a_4$

(d) $-a_2$ (e) $+a_2$ (j) $-a_5$ (k) $+a_5$

(f) $-a_3$ (g) $+a_3$ (l) $-a_6$ (m) $+a_6$

Figure 3.8.: Overview of the effects of fit coefficients a_1 to a_6 on a second-order surface (see Equation Equation 3.3). Subfigure 3.8a shows the basic surface with coefficients a_1 to a_6 set to zero and the gray scale used to improve depth perception. Subfigures 3.8b to 3.8m then show the resulting surfaces for isolated negative (-) or positive values (+) of each of the six coefficients a_1 to a_6.

bigger horizontal gaze displacements, a_6 is positive (3.8m). Finally the amount of surface twist can be measured by the coefficient a_5, which is thus commonly named the *twist score* [Glenn and Vilis, 1992]. If this coefficient is negative, the eye rotates counterclockwise for gazes to the upper left and lower right and it rotates clockwise for looks to the upper right and lower left (3.8j). In the opposite case, twist score a_5 is positive (3.8k).

3.4.6. Statistics

If not noted otherwise, data were summarized by means and standard deviations ($M \pm SD$). A Lilliefors test of the null hypothesis that data come from a distribution in the normal family was done on the samples. Depending on confirmation or rejection of this null hypothesis, Student's t-test or Wilcoxon's rank-sum test were used for statistical analysis. The Pearson product-moment correlation coefficient or Pearson's r is reported as a measure of correlation. Statistical significance was set at $p < 0.05$.

4. Results

A number of neurophysiological studies have focused on the behavioural constraints that reduce the redundant degrees of freedom of the eye and the head during visual fixation in order to decrease the number of neural control parameters and simplify the coordination of gaze movements (see Background section 2.3.2). Nonetheless, it remains unclear whether torsional constraints are independent of the direction of the saccade preceding the current fixation in combined eye and head gaze shifts. In this chapter, simultaneous eye and head movements are analyzed so as to compare constraints of torsion for different initial gaze positions.

4.1. Donders' Law in the Star Paradigm

This section describes the torsional constraints of repeated eye-head gaze shifts with a single origin per gaze target. The data serve as control data for the following comparison with the Diamond paradigm recordings.

4.1.1. Qualitative Description

The two main implications of Donders' law can qualitatively be demonstrated by simple plots of the torsional components of gaze, head and eye. Figure 4.1 shows three-dimensional motion records of the three body units in a single subject during three gaze shifts to the lower left target position (marks 1-3) and one gaze shift to the upper left target position (mark 4). The movements can easily be recognized in the two-dimensional projections

on the frontal plane as seen from in front of the subject (4.1d, 4.1f, 4.1h). All four trials started at straight-ahead gaze and were not executed in sequence during the Star paradigm. The individual horizontal and vertical components of these frontal projections are plotted over time in Subfigures 4.1a and 4.1b. The torsional components (4.1b) become visible in sagittal projections, as data are seen from the right side of the subject (4.1e, 4.1g, 4.1i).

The first implication of Donders' law is that torsional orientations of gaze, head and eye *are* constrained for unique horizontal-vertical orientations. The torsional traces (4.1c) are stable during fixations (solid line segments in 4.1b, 4.1a) and only change values during saccadic movements (dotted line segments). So for example, torsion of gaze was always -11.69 $\pm$ 0.59 deg during the three fixations on the lower left visual target in 4.1c. Head (-4.12 deg $\pm$ 0.36 deg) and eye torsion (-10.51 deg $\pm$ 0.47 deg) were constrained with even less variation during the exemplary fixations. These torsional constraints may seem evident but are not, considering that no specific torsional gaze, head or eye orientation is necessary to look at a visual target defined only by horizontal and vertical retinal coordinates.

Secondly, the torsion of gaze, head and eye is constrained to *specific* orientations for any unique horizontal-vertical orientation. This can best be seen in the sagittal projections 4.1e, 4.1g, and 4.1i and also in torsion over time 4.1c. Whereas the gaze shifts to the lower left (1-3) resulted in counterclockwise torsion of the body units, the gaze shift to the upper left target position (4) resulted in clockwise rotations of gaze (12.68 deg $\pm$ 0.78 deg), head 1.47 deg $\pm$ 0.08 deg) and eye (8.01 deg $\pm$ 0.75 deg).

With this, Figure 4.1 gives a brief overview and some hints, as to the torsional constraints of combined eye-head gaze shifts. However, to qualitatively and quantitatively describe the shown torsional constraints of not only a few selected gaze orientations but for all fixation samples simultaneously, the recorded data have to be analyzed in a more abstract way. The following section will take you through an abstraction leading to a quantitative description of the torsional constraints in the Star paradigm recordings in order to parametrically compare them with the Diamond paradigm recordings in the next chapter.

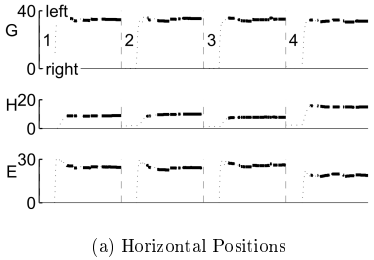

(a) Horizontal Positions

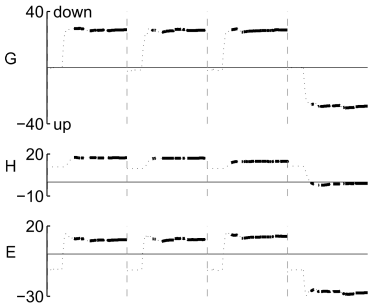

(b) Vertical Positions

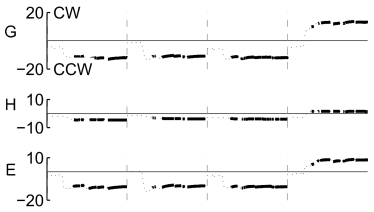

(c) Torsional Positions

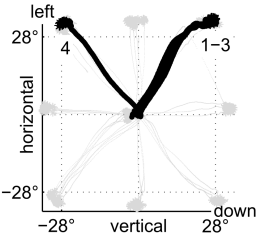

(d) Gaze (front)

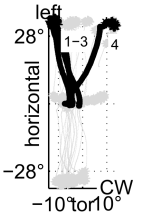

(e) Gaze (side)

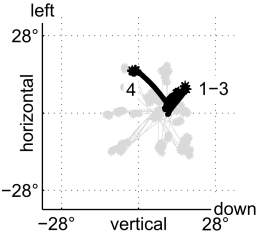

(f) Head (front)

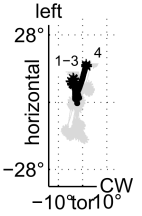

(g) Head (side)

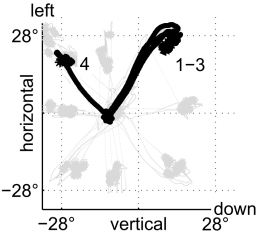

(h) Eye (front)

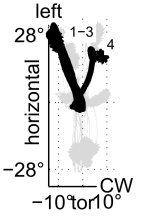

(i) Eye (side)

Figure 4.1.: Star paradigm: Horizontal, vertical and torsional (4.1a-4.1c) orientations (deg) of gaze (G), head (H) and eye (E) plotted over time for 4 selected trials (Subject: BB). Fixations highlighted as thick, solid line segments. Trials marked 1-4 in 2D back/side projections of the complete recording for gaze (4.1d/4.1e), head (4.1f/4.1g) and eye (4.1h/4.1i). CW, clockwise; CCW, counterclockwise.

4.1.2. Second Order Surface Fits

As it can be seen from the previous section, the ranges of the recorded fixation samples for gaze, head and eye are constrained in torsional direction. According to Donders' law in a next step of abstraction we expect all fixation samples of each body unit (gaze, head or eye) over an entire experiment recording to come to lie on a three-dimensional surface. To quantify the shapes of these surfaces we fitted second-order surfaces to the quaternion data as described in Methods section 3.4.4.

Figure 4.2 shows the resulting surfaces of gaze (4.2a), head (4.2b) and eye (4.2c) for a complete Star paradigm recording in a single subject. For a better visualization of the three-dimensional properties of the surfaces, their contours are cast onto three sides of the enclosing coordinate boxes and the aspect of the torsional axes is zoomed to double the torsional resolution of the plots. The thick lines in the projections of the surface contours represent the fit coefficients a_2 and a_3. To clarify the relation of the recorded position samples and the fitted second-order surface, subfigure 4.2a shows not only the gaze surface, but also the respective three-dimensional gaze fixation samples.

Corresponding to the second order formula in Equation 3.3 the surface in Figure 4.2 visualizes the dependence of torsional orientations on the respective horizontal and vertical position components of gaze, head and eye. Figure 4.3 shows the statistics of these relations over all seven subjects in form of box plots. In the three subfigures one box per coefficient (a_1 to a_6 in Equation 3.3) is plotted for the surfaces fitted to gaze (4.3a), head (4.3b) and eye (4.3b). Means and standard deviations of each of the surface fit coefficients a_1 to a_6 over all subjects can be found in Table 4.1. The following paragraphs give short descriptions of the six coefficients.

Coefficient a_1 None of the three body units had a torsional offset. Over all subjects the coefficient a_1 values were grouped closely together and did not differ significantly from zero (Figure 4.3 and Table 4.1). That is there was no global tendency of rotatory segment displacement in any torsional direction (clockwise or counterclockwise). This can be visu-

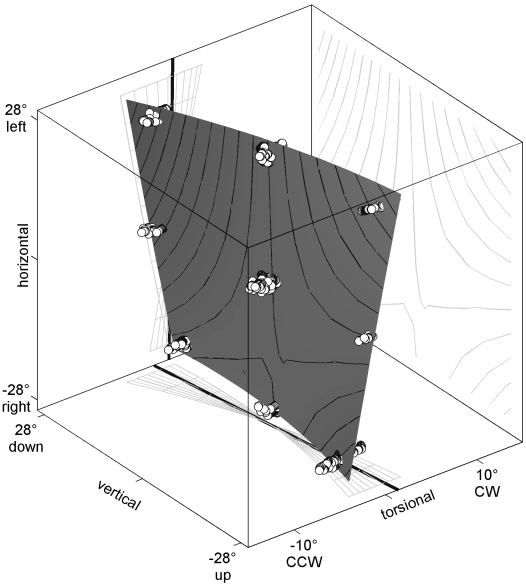

(a) Gaze

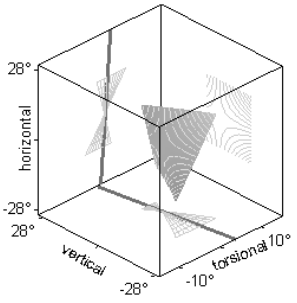

(b) Head

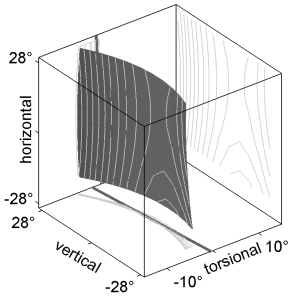

(c) Eye

Figure 4.2.: 2nd-order surface fits for a complete Star paradigm recording (subject: BK). Surface contours are cast onto 3 sides of the enclosing boxes. Thick lines in the contours represent fit coefficients a_2 (bottom) and a_3 (side). Aspect ratio of torsional to horizontal/vertical axes is 2:1.

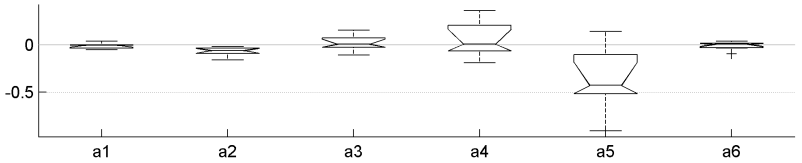

(a) Gaze

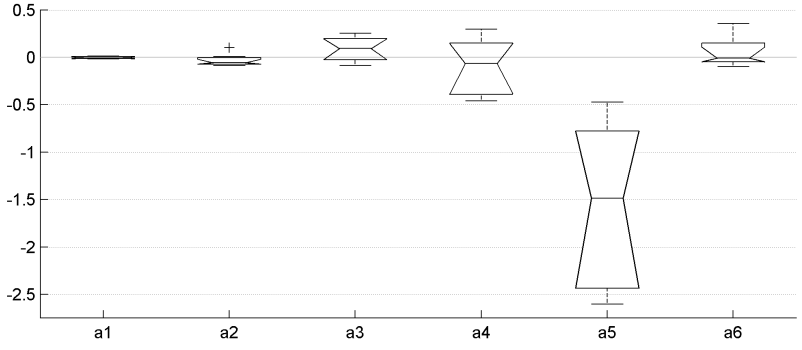

(b) Head

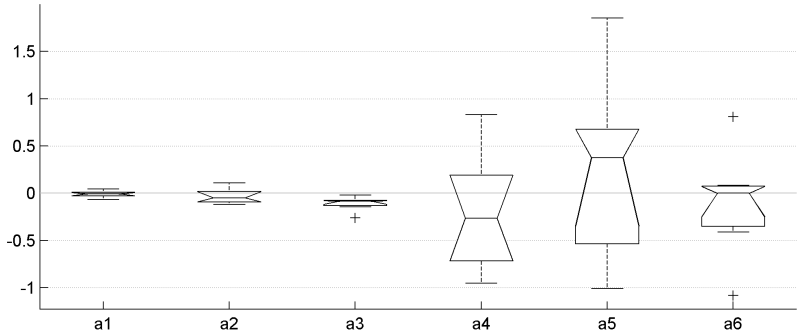

(c) Eye

Figure 4.3.: Star paradigm: Surface coefficients (n=7). Boxes represent median (center line), 25th/75th percentiles (edges) and extremes (whiskers). Outliers (+) lie outside ± 2.7 SD. Notches show uncertainty of medians at 5% significance.

ally confirmed in the plots of the exemplary subject: Neither the gaze (4.2a: $a_1 = 0$), head (4.2b: $a_1 = 0.01$) nor eye surface (4.2c: a_1 = -0.02) were torsionally displaced.

Coefficient a_2 The gaze surface had a negative torsional slope a_2 for vertical displacements ($p < 0.02$); for the head and the eye this slope did not significantly differ from zero (Figure 4.3 and Table 4.1). Thus, the eye-in-space exhibited counterclockwise rotation when the line of sight was directed downwards and it exhibited clockwise rotation when the subjects looked up. In the gaze surface plot of the example subject (4.2a), this behavior is marked by the thick line in the bottom projection (a_2 = -0.06). Here, the head (4.2b: a_2 = -0.07) and less markedly the eye surface (4.2c: a_2 = -0.04) have a negative slope as well.

Coefficient a_3 Surface slopes a_3 for horizontal displacements tended to have positive values for the head and were significantly lower than zero for the eye ($p < 0.01$); for gaze the a_3 coefficient did not significantly differ from zero (Figure 4.3 and Table 4.1). Looking at the thick slope lines in the side projections of the example surface contours (Figure 4.2) this means: There was no gaze torsion for horizontal gaze shifts (4.2a: $a_3 < 0.01$), but the head rotated clockwise when looking left and counterclockwise when looking right (4.2b: a_3 = 0.04) whereas the eyes counter-rolled into the respective other torsional direction (4.2c: a_3 = -0.02).

Coefficient a_4 None of the surfaces were torsionally curved in relation to vertical orientation. Since a_4 and the following coefficients a_5 and a_6 are quadratic, they scatter over a considerably larger range than the related linear coefficients a_1 to a_3. Still over all subjects neither a_4 for gaze, head or eye differed significantly from zero (Figure 4.3 and Table 4.1). The subject of the example plots in Figure 4.2 exhibited some curvature on the eye surface and so the eye rotated counterclockwise for peripheral vertical positions in both upward and downward gaze (4.2c: a_4 = -0.49). In contrast, example surfaces for gaze (4.2a: a_4 = -0.19) and head (4.2b: a_4 = -0.20) were not curved for vertical excursions.

Coefficient a_5 Gaze and head surfaces were twisted, whereas eye surfaces were twist-free planes (see also coefficients a_4 and a_6). From the example surface plots of gaze (4.2a) and head (4.2b) it is understandable, why Glenn and Vilis coined the term *twist score* [Glenn and Vilis, 1992]. Negative a_5 coefficients make the second-order surfaces of gaze (a_5 = -0.43) and head (a_5 = -2.49) twist, as if they were square sails attached between top and bottom beams rotated in opposite directions. This can also be clearly seen from the side and bottom projections in 4.2a and 4.2b in that the surface twist makes the contours appear to fan out from the center like bow-ties. The example eye surface (4.2c) was twist-free ($a_5 = 0.07$). Over all subjects, a_5 coefficient values were significantly lower than zero for both gaze ($p < 0.05$) and head ($p < 0.01$) and did not significantly differ from zero for the eye (Table 4.1).

Coefficient a_6 Just as with coefficient a_4, none of the surfaces showed an overall tendency to curve at the horizontal edges. There was only negligible bend at the horizontal edges in the surface plots of our example subject: a_6 is 0.05 for gaze (4.2a), -0.01 for the head (4.2b) and 0.09 for the eye (4.2c). The a_6 box plots in Figure 4.3 reflect this observation over all subjects: a_6 coefficients were closely grouped and none of them was significantly different from zero (see also Table 4.1).

4.1.3. Torsional Thickness

Having characterized the torsional constraints of gaze, head and eye movements in the previous section, it is necessary to provide a description of their variability. The standard deviation of the torsional residuals about the fitted second-order surfaces is a measure of how closely the recorded movement samples adhere to the constraints implied by the surface function. It is also often pictorially called the *torsional thickness* of those surfaces.

Figure 4.4 juxtaposes the values of torsional thickness of the seven subjects for each of the three segments gaze, head and eye (subfigures 4.4a, 4.4b and 4.4c) in the Star paradigm recordings. The last grayscale bar in each of the three subfigures represents the mean for

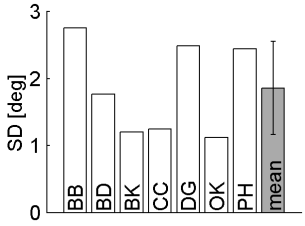

(a) Gaze

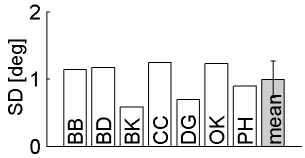

(b) Head

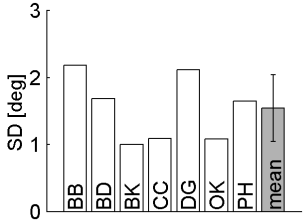

(c) Eye

Figure 4.4.: Star paradigm: Torsional thickness values of each of the seven subjects. Grayscale bars at the right are the means; whiskers demarcate the standard deviations.

the respective diagram and its whiskers demarcate the standard deviation. As it can be seen from these plots, there are consistent differences in the torsional thickness of the surface fits for gaze, head and eye. The thinnest surfaces, if you will, can be found in the head rotation data (4.4b) with a mean torsional thickness of 1.00 deg $\pm$ 0.27 deg. Eye surfaces (4.4c) were significantly thicker for all subjects ($p = 0.02$) with a mean torsional variation of 1.54 deg $\pm$ 0.50 deg. Finally the torsional thickness of the gaze data (1.86 deg $\pm$ 0.70 deg; 4.4a) was bigger than the variation range of the torsional eye data. This difference, was also statistically significant over all subjects ($p = 0.01$). Therefore, in each case the torsional thickness of gaze was bigger than the torsional variation of the eye, which in turn was bigger than that of the head.

Coefficient	Gaze	Head	Eye
	Mean ± SD (n = 7)		
a_1	-0.01 ± 0.03	0.00 ± 0.01	-0.01 ± 0.03
a_2	**-0.07 ± 0.05**	-0.03 ± 0.07	-0.03 ± 0.08
a_3	0.02 ± 0.08	0.09 ± 0.13	**-0.11 ± 0.08**
a_4	0.05 ± 0.19	-0.09 ± 0.30	-0.19 ± 0.62
a_5	**-0.36 ± 0.35**	**-1.58 ± 0.88**	0.25 ± 0.95
a_6	-0.01 ± 0.04	0.05 ± 0.16	-0.10 ± 0.57

Table 4.1.: Star paradigm: Coefficients $a1$ - $a6$ for the second-order surface fits to torsional gaze, head and eye orientations. Values that significantly differ from zero are in bold font ($p < 0.05$).

4.2. Donders' Law in the Diamond Paradigm

In this section the analysis of torsional constraints is repeated for the Diamond paradigm recordings. In this paradigm, every visual target is fixated four times with different directions of the preceding eye-head gaze saccades.

4.2.1. Qualitative Description

Figure 4.5 qualitatively demonstrates torsional constraints of gaze, head and eye during four independent gaze shifts to the lower left target position that all start from *different* initial orientations. Origins of the trials at the middle, left and right upper target positions (1-3) and at the central target position (4) are numbered in all subfigures. The order of trials does not represent their actual sequence during recording.

Torsional constraints were evident in the presentation of the torsional data components as a function over time (4.5c): For the common end target of the four trials (lower left target position marked by x e.g. in 4.5d), regardless of the initial eye-head gaze position (1 - 4), the brain always selected the same torsional orientation of gaze, head and eye. In the subject shown, this orientation was -7.99 deg $\pm$ 1.09 deg torsion for the gaze, -0.46 deg $\pm$ 1.23 deg for the head and -5.62 deg $\pm$ 1.03 deg for the eye, consistently over the four trials. Two-dimensionally this behavior can best be visualized in the gaze plot (4.5e) since it has the biggest torsional amplitudes: In the four selected trials, gaze orientations at the pre-step fixation target differ by several degrees of torsion: -0.52 deg at mark 1, 0.55 deg at mark 2, -6.14 deg at mark 3, and -3.42 deg at mark 4. Nonetheless, gaze shifts always ended at the same single torsional orientation (-7.99 deg $\pm$ 1.09 deg; mark x).

We will now follow the same approach as in the previous chapter in extracting more abstract quantitative features from the recorded data to finally be able to compare the results of the Star and Diamond paradigms.

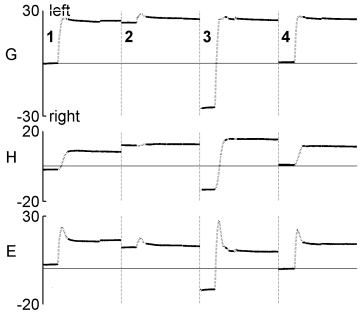

(a) Horizontal Positions

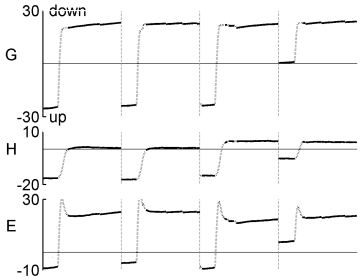

(b) Vertical Positions

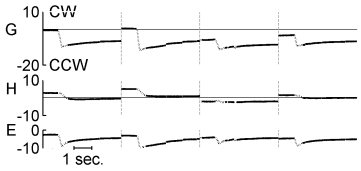

(c) Torsional Positions

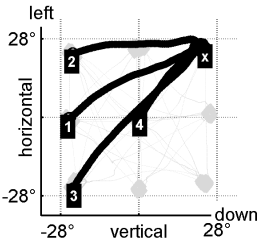

(d) Gaze (back)

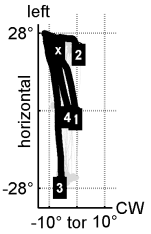

(e) Gaze (side)

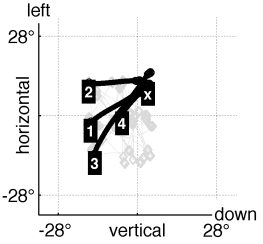

(f) Head (back)

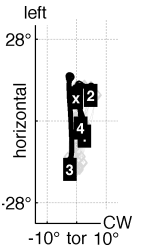

(g) Head (side)

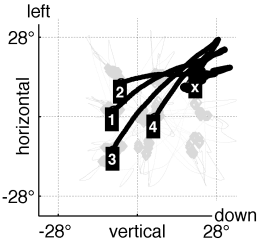

(h) Eye (back)

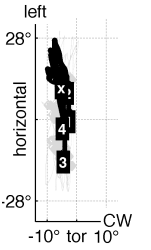

(i) Eye (side)

Figure 4.5.: Diamond paradigm: Raw horizontal, vertical and torsional positions (4.5a-4.5c) of gaze (G), head (H) and eye (E) as functions of time for 4 selected trials (Subject: BK). Fixations as thick solid line segments. Trace data marked in 2D back/side projections of the complete recording for gaze (4.5d/4.5e), head (4.5f/4.5g) and eye (4.5h/4.5i). CW, clockwise; CCW, counterclockwise.

4.2.2. Second Order Surface Fits

Figure 4.6 shows second order surfaces of an exemplary subject that are fitted to the quaternion data of gaze (4.6a), head (4.6b) and eye (4.6c). Figure 4.7 shows the statistics for the six surface fit coefficients as box plots and Table 4.2 lists their values.

Coefficient a_1 None of the three surfaces in Figure 4.6 showed a torsional offset (a_1 for gaze: -0.03, head: 0.01, eye: -0.04). Also, over all subjects the box plots in Figure 4.7 showed closely grouped a_1 coefficients that did not differ significantly from zero (Table 4.2).

Coefficient a_2 For vertical displacements torsional slope a_2 was negative in gaze ($p < 0.02$) and did not differ significantly from zero in head and eye (Figure 4.7 and Table 4.2). The example subject shown in Figure 4.6 rotated his eye-in-space (gaze) counterclockwise when looking down and clockwise when looking up (thick blue line in bottom contour in subfigure 4.6b: a_2 = -0.05). He did the same with the head (4.6a: a_2 = -0.10) and negligibly with the eye (4.6c: a_2 = -0.01).

Coefficient a_3 The a_3 eye coefficients clustered closely and were significantly lower than zero. On the other hand, a_3 head coefficients spread over a larger range and had a non-significant tendency to positive values. The values for all the a_3 gaze coefficients were grouped around zero (Figure 4.7 and Table 4.2). The example subject (Figure 4.6) did not show considerable deviations from zero in any of the three a_3 coefficients (gaze: 0.00, head: -0.03, eye -0.02).

Coefficient a_4 As coefficient of a squared term, a_4 scattered over a larger range than the three preceding linear coefficients a_1 to a_3 but was not significantly different from zero for any segment (Figure 4.7 and Table 4.2). In the example subject (Figure 4.6) there was a slight tendency towards counterclockwise rotations for peripheral vertical eye positions (a_4 for eye: -0.46, for gaze: -0.16 and for head: -0.12).

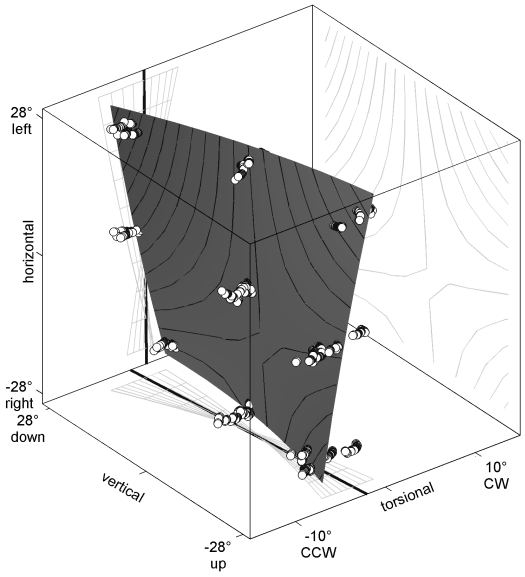

(a) Gaze

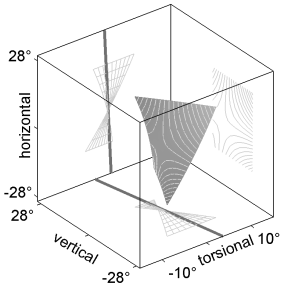

(b) Head

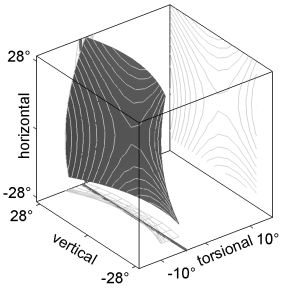

(c) Eye

Figure 4.6.: 2nd-order surface fits for a complete Diamond paradigm recording (subject: BK). Surface contours are cast onto 3 sides of the enclosing boxes. Thick lines in the contours represent fit coefficients a_2 (bottom) and a_3 (side). Aspect ratio of torsional to horizontal/vertical axes is 2:1.

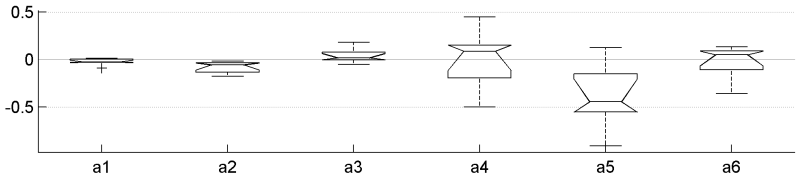

(a) Gaze

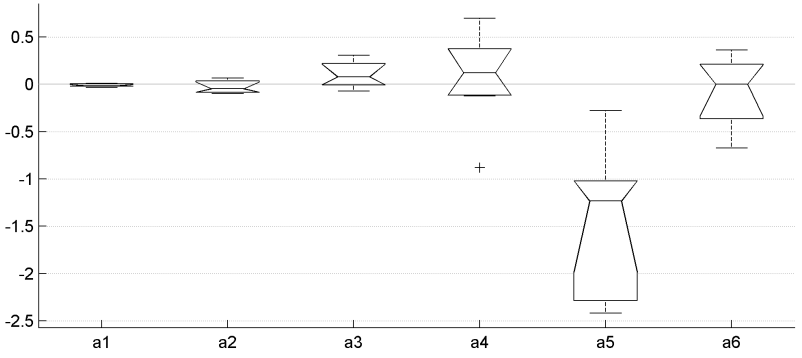

(b) Head

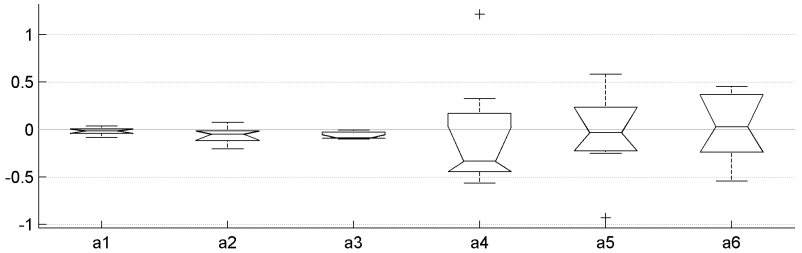

(c) Eye

Figure 4.7.: Diamond paradigm: Surface coefficients (n=7). Boxes show median (center line), 25th/75th percentiles (edges) and extremes (whiskers). Outliers (+) lie outside ± 2.7 SD. Notches show uncertainty of medians at 5% significance.

Coefficient a_5 Again the surfaces for gaze and head were significantly twisted (Figure 4.7 and Table 4.2; $p < 0.02$). This can also be seen in the example surfaces for gaze (4.6a: a_5 = -0.47) and head (4.6b: a_5 = -2.29). The eye surface in contrast was twist-free over all subjects and also in the example subject (4.6c: a_5 = 0.28).

Coefficient a_6 Finally, over all subjects there was no torsional curve related to peripheral horizontal positions in any of the three segments (Figure 4.7 and Table 4.2). The example subject followed this statistic in his a_6 gaze coefficient (4.6a: a_5 = 0.05), but exhibited a little negative bend at the horizontal edges of the head surface (4.6b: a_6 = -0.29) and a slightly positive bend at the horizontal edges of the eye surface (4.6c: a_6 = 0.35).

4.2.3. Torsional Thickness

Figure 4.8 gives a quantitative control of quality of the surface fits from the preceding section. It plots the torsional thickness values (standard deviation of torsional residuals) of every subject for gaze (4.8a), head (4.8b) and eye (4.8c). Again the head surfaces were the thinnest (4.8b: 1.24 deg $\pm$ 0.37 deg) followed by the eye surfaces (4.8c: 1.78 deg $\pm$ 0.86 deg). The torsional thicknesses of the gaze surfaces significantly were the biggest (4.8a: 2.10 deg $\pm$ 0.80 deg; $p < 0.01$).

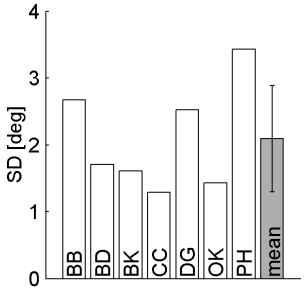

(a) Gaze

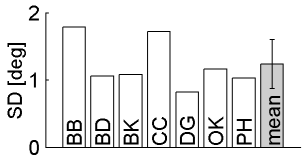

(b) Head

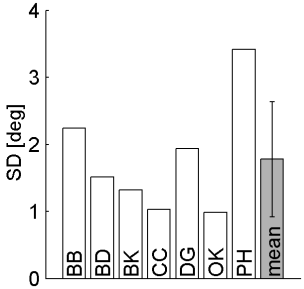

(c) Eye

Figure 4.8.: Diamond paradigm: Torsional thickness values of each of the seven subjects. Rightmost bar in every subfigure represents the mean; whiskers demarcate the standard deviation.

Coefficient	Gaze	Head	Eye
	Mean ± SD (n = 7)		
a_1	-0.02 ± 0.03	-0.01 ± 0.02	-0.02 ± 0.04
a_2	**-0.08 ± 0.06**	-0.02 ± 0.07	-0.06 ± 0.09
a_3	0.04 ± 0.08	0.10 ± 0.14	**-0.06 ± 0.04**
a_4	0.00 ± 0.31	0.05 ± 0.50	-0.07 ± 0.64
a_5	**-0.38 ± 0.33**	**-1.52 ± 0.82**	-0.06 ± 0.48
a_6	-0.02 ± 0.17	-0.08 ± 0.38	0.04 ± 0.38

Table 4.2.: Diamond paradigm: Coefficients $a1$ - $a6$ for the second-order surface fits to torsional gaze, head and eye orientations. Values that significantly differ from zero are in bold font ($p < 0.05$).

4.3. Donders' Law: Star vs. Diamond Paradigm

In this section the torsional constraints observed between combined eye and head gaze saccades with *different* directions per target (Diamond paradigm) are compared to the torsional constraints of the control condition, where all gaze shifts to a single target had the *same* direction (Star paradigm).

By means of exploratory data analysis Figure 4.9 reveals that the shapes of the second-order surfaces fitted to gaze (4.9a), head (4.9b), and eye (4.9c) did not differ significantly between the two paradigms. The figure juxtaposes the box plots of surface fit coefficients a_1 to a_6 for the Star paradigm (grayscale boxes) and the Diamond paradigm (colored boxes). Notches in the boxes mark the 95% confidence intervals for the box medians. Thus, the box plots, whose notches do not overlap, would have different medians at the 5% significance level. In contrast, the notches in all couples of coefficient boxes in Figure 4.9 did overlap.

The 5% significance level is based on a normal distribution assumption, but comparisons of medians are reasonably robust for other distributions as well. Moreover, Lilliefors tests showed no significant deviations from a normal distribution for all but the following between-subjects coefficient samples: coefficients a_2 and a_6 of the head in Star paradigm, as well as coefficients a_2 of the gaze and coefficients a_3 and a_4 of the eye in the Diamond paradigm. Analogously to this visual hypothesis test in Figure 4.9, paired-samples t-tests or Wilcoxon signed rank tests for the not normally distributed coefficients showed not a single significant difference between surface fit coefficients of the Star and Diamond paradigm.

In Figure 4.10 it is assessed, whether the recorded data adhere as closely to the fitted surfaces for the Diamond paradigm as for the Star paradigm. For each of the three body units (gaze 4.10a, head 4.10b, and eye 4.10c), a paired t-test difference plot visualizes the relationship between the torsional thicknesses in the two paradigms: The difference between the torsional standard deviations in the Diamond and Star paradigms is plotted on the y-axis and the mean of the two torsional standard deviations is plotted on the x-axis. Dots above the horizontal zero line (dashed, gray) represent subjects who showed higher

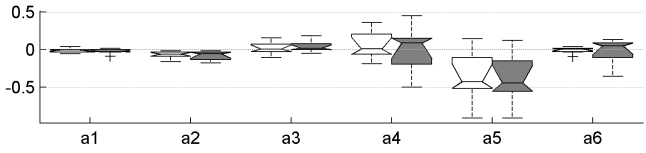

(a) Gaze

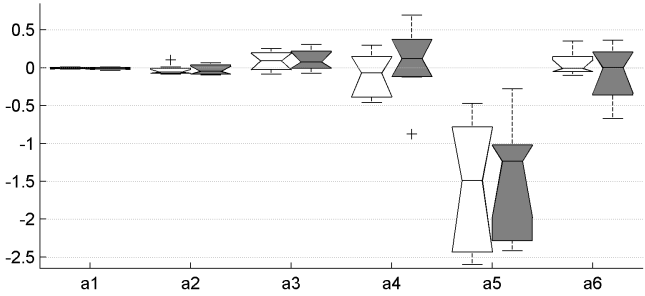

(b) Head

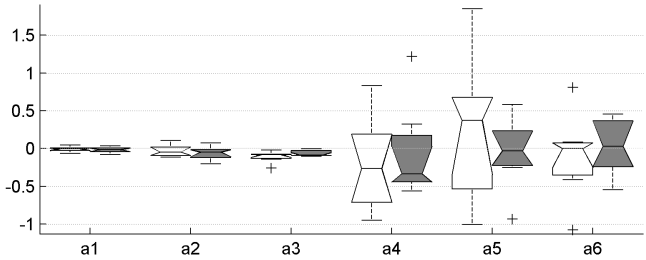

(c) Eye

Figure 4.9.: Star (empty boxes) vs. Diamond (grayscale boxes) paradigm: Surface fit coefficients $a1$ - $a6$ (n = 7). Boxes have lines at the lower quartile, median and upper quartile coefficient values. Whiskers extend from end of box to adjacent most extreme values. Notches in the boxes represent a robust estimate of the uncertainty about the medians at the 5% significance level. There were no significant differences between Star and Diamond paradigms for any of the coefficients a_1 - a_6 (all notches of the coefficient box couples overlap).

torsional variability in the Diamond paradigm than in the Star paradigm. Conversely dots below the zero line stand for subjects who torsionally deviated more from the fitted surface constraints in the Star paradigm than in the Diamond paradigm. Ideally, all points would fall along the zero line, indicating that on average intra-subject variability of torsion about the fitted surfaces was equal in the two paradigms. To decide whether this was the case, each plot in Figure 4.10 shows the 95 % confidence interval of the mean of SD differences above and below the mean line. Since in each of the plots the zero line lies within this confidence interval, there were no significant differences between Star and Diamond paradigm in torsional thickness for gaze, head or eye.

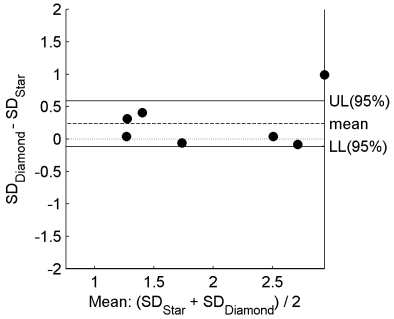

(a) Gaze

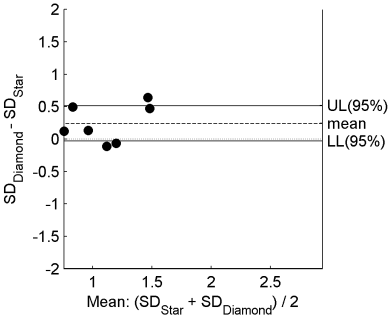

(b) Head

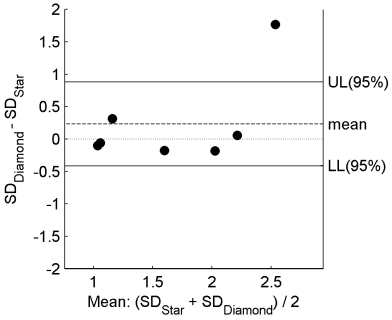

(c) Eye

Figure 4.10.: Star vs. Diamond paradigm: Paired t-test difference plots of torsional thickness. Every point shows the difference vs. the mean of the paired torsional thickness values (Star/Diamond) in a single subject. The 95 % confidence interval of mean difference above (UL) and below (LL) the black dashed mean line hint whether the mean differs significantly from zero (gray dashed line) or not. All units in degrees.

4.4. Correlations of Eye and Head Torsion

In this last results section the correlations between torsional variability of head and eye orientations are analyzed. Implications on the interdependencies of eye and head movement control during head-unrestrained gaze shifts are presented in the Discussion.

Figure 4.11 illustrates that between subjects, the torsional variabilities of head and eye orientations were independent of each other. Torsional residuals of fixations on each of the nine target position were calculated individually for head and eye in all subjects. Residuals were defined as the differences between the torsional fixation samples and their mean value for the respective target position. Next the coefficients of correlation between the torsional residuals of head and eye were determined for the individual subjects. For the Star paradigm these correlations were significant within every subject. For the Diamond paradigm the correlations were not significant in four of the seven subjects ($p < 0.6$) . Boxes in Figure 4.11 plot medians and quartiles of the correlation coefficients over all subjects and separated by paradigm. Although *within* most subjects the correlations of torsional variabilities in eye and head orientation were significant, the correlations did not differ significantly from zero *between* subjects both for the Star and Diamond paradigm.

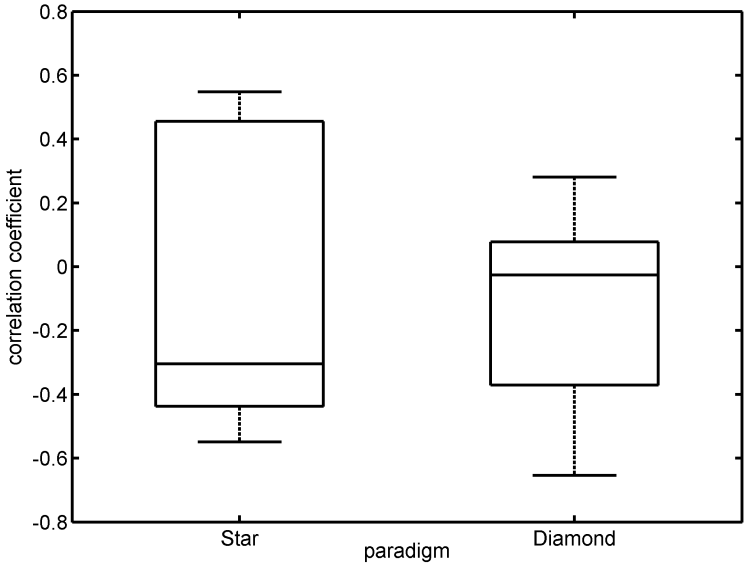

Figure 4.11.: Correlation coefficients between the torsional residuals of head and eye fixations for the Star and Diamond paradigm over all 7 subjects. Boxes have lines at the lower quartile, median and upper quartile coefficient values. Whiskers extend from each end of the box to the adjacent most extreme coefficients.

5. Discussion

The aims of this study were to see whether Donders' law holds after head-unrestrained saccades, independently of the saccade direction, and whether head and eye control are dependent or independent at this. The secondary objective was to describe control data from healthy adults for comparison in clinical studies. Thus, this chapter starts out with a short discussion of the observed torsional constraints and then describes the comparison between the Star and Diamond paradigms. In the third section, the correlations of head and eye torsion are discussed in relation to the interdependencies of head and eye movement control. Finally, an outlook on the clinical application of three dimensional head and eye recordings is given by example of a recent study.

5.1. Torsional Constraints of Eye-Head Saccades

In this study torsional constraints of gaze, head and eye were quantified by fitting second order surfaces to the respective three-dimensional orientation samples. This approach yields six coefficients for every fit (Tables 4.1 and 4.2), each of which quantifies some aspect of surface geometry [Glenn and Vilis, 1992, Medendorp et al., 1998, Crawford et al., 1999]. In the following paragraphs the implications for torsional gaze, head and eye movement constraints are discussed.

An overall torsional offset of the gaze, head or eye orientations is given by the a_1 term. Since during calibration this parameter is set to zero, a_1 values for all three body units never significantly differed from zero.

Torsion occurring with vertical excursions of a body unit is described by the a_2 term. In

both paradigms a_2 values did not significantly differ from zero for the head and the eye. For gaze, the a_2 values were small but always negative. This could reflect a weak tendency of gaze to roll clockwise when facing up and counterclockwise when facing down. However, the coefficient a_2 values of gaze (Star paradigm: -0.07; Diamond paradigm: -0.08) were as small that the resulting torsional deviations even for large vertical excursions of 28 deg amplitude ($-0.08 * \pm 28deg = \mp 2.24deg$) were well within the torsional thickness of the gaze surface (Diamond paradigm: 2.10 $\pm$ 0.80 deg). Nonetheless, in subjects with a large vertical eye motion range, the possibility of measuring artifacts, due to the exiting wire of the search coil touching the upper eyelid, can not be totally disregarded (see [Bergamin et al., 2004]).

Coefficient a_3 values measure torsion in relation to horizontal movements. For gaze and head they never significantly differed from zero. For the eye all a_3 values were negative (Star paradigm: -0.11; Diamond paradigm: -0.06). These negative scores describe a backward tilt of the eye displacement surfaces in the head, which reflects the tendency of the eye to roll clockwise when facing right and counterclockwise when facing left. This pattern is well known during activation of the otolith organs, e.g. by a static head or body pitch forward [Crawford and Vilis, 1991, Haslwanter et al., 1992]. Correspondingly, during the recordings most of the subjects let their head hang slightly forward, when no more large vertical head excursions were demanded after the calibration.

Coefficient a_4, in contrast to coefficient a_2, describes increasing torsion in only one direction for any upward or downward vertical excursion. Its values for gaze, head and eye did not significantly differ from zero. Hence between subjects the fitted surfaces had no curvature along the torsional axis with vertical gaze, head or eye position.

Accordingly, torsional surface curvature with horizontal positions is described by coefficient a_6. It, too, never significantly differed from zero.

The amount of surface twist measured by a_5 was significantly different from zero for the head in that all individual a_5 values were negative. This indicates that the head moves like a gimbal, having a horizontal axis nested within a space-fixed vertical axis. Any such gimbal is called a Fick gimbal [Glenn and Vilis, 1992, Radau et al., 1994]. Both [Ceylan et al., 2000] and [Medendorp et al., 1998] report all negative twist scores for the

head as well (-1.34 to -0.29 and -1.13 to -0.28). Also, [Glenn and Vilis, 1992] measured head position data that resulted in a twist score significantly smaller than zero (-0.68 ± 0.21). [Radau et al., 1994] experimented with standing subjects where they found a twist score of the head relative to the chest of -0.94 ± 0.32 (a_5 of the head relative to space was -1.45 ± 0.30). In the results presented for this thesis, the twist scores of gaze are significantly lower than zero. When [Glenn and Vilis, 1992] first stated that the eye-in-space (gaze) surface resembled that of a Fick gimbal, they report concordant a_5 values (-0.64 ± 0.09). [Radau et al., 1994] described an even more prominent negative twist score for the gaze (-1.23 ± 0.18). The only a_5 values that did not indicate a twisted surface were the scores for the eye-in-head. This planar eye displacement surface is the so called Listing's plane [Helmholtz, 1867, Westheimer, 1957, Ferman et al., 1987, Tweed and Vilis, 1990]. Again [Glenn and Vilis, 1992] reported a comparable range of a_5 eye values from -1.03 to 0.91 and [Radau et al., 1994] stated an eye twist score of -0.64 ± 1.59.

In sum this thesis not only provides a comprehensive description of all surface fit coefficients for gaze, head and eye in healthy human subjects, but also the reported values are in a good agreement with the subset of coefficient values that has been detailed in earlier publications. In particular all parameters of the head both in the Star and in the Diamond paradigm were in accordance with the report of head coefficient values by [Ceylan et al., 2000].

Torsional Thickness Deviations from Donders' law in our recordings were rather small as it becomes evident when comparing the torsional thickness of the fitted surfaces with those reported in other studies: Between the three body units, unanimously gaze (eye in space) exhibited the biggest variability of torsional residuals around the fitted second-order surfaces. For this study the torsional thickness of the gaze surface averaged over Star and Diamond paradigm amounted to 1.66 deg ± 0.61 deg. Other reports ranged from a mean gaze surface thickness of 2,9 deg [Tweed et al., 1995], over a span from 1.21 deg to 3.42 deg [Radau et al., 1994] to 3.26 deg ± 0.62 deg [Glenn and Vilis, 1992]. These differences may partly be due to different visual target array extents. All three cited studies used

considerably larger arrays than this study with target eccentricities between 70 deg and 135 deg.

Eye (in head) surfaces in this study had the second largest torsional variation of 1.66 deg ± 0.61 deg over torsional thickness of the head of 1.12 deg ± 0.29 deg. Accordingly, [Radau et al., 1994] reported 2.62 deg ± 0.80 deg torsional thickness for the eye and 1.10 deg ± 0.27 deg for the head. In two other studies, ranges of torsional variability for head and eye were similar, but with deviations of the eye being smaller than those of the head: [Glenn and Vilis, 1992] reported 2.40 deg ± 0.92 deg for eye and 2.56 deg ± 0.53 deg for the head; [Tweed et al., 1995] 1.9 deg (eye) and 2.6 deg (head). Again the differences may at least in part be attributed to a key difference in the experimental setups: The latter two studies eliminated changes in vergence angle between the subject's eyes by presenting the visual targets on an isovergence dome. On the other hand, for the study of [Radau et al., 1994], as well as for this thesis, changes in vergence angle were minimized by placing the targets close to optical infinity. Here, residual small vergence changes (< 0.5 deg) may occur that provoke slight rotations of Donders' surface of the eye-in-head during recording and thus resulted in an increased torsional thickness of the eye surface [Allen and Carter, 1967, Van Rijn and Van den Berg, 1993, Bruno and van den Berg, 1997, Kapoula et al., 1999, Steffen et al., 2000].

Overall it can be concluded that after head-unrestrained gaze saccades under the Star and Diamond paradigm, torsional orientations of both gaze, head and eye each are constrained to three-dimensional displacement surfaces. Thereby, each body unit follows an individual form of Donders' law: The head surface has a pronounced twist, whereas the eye surface is flattened like a plane (Listing's plane); the gaze surface has an intermediate twist between those of head and eye. Adherence to these constraints is closest for the head, followed by the eye and finally by gaze with the biggest torsional thickness. The results obtained with our recording technique and analysis are in line with data reported in literature. By this, conclusions drawn in this thesis have a strong base of evidence and the reported data set forms a valid control for comparisons with patient data of eye-head coordination in clinical research and applications.

5.2. Validity of Donders' Law for Different Initial Eye-Head Gaze Positions

For a steady fixation of distant targets with the head fixed and upright, Donders' law states that for any unique gaze direction, regardless of how it was reached by the eye, the brain always selects the same eye orientation in three-dimensional space [Donders, 1848]. It has been suggested that Donders' law holds not only with the head fixed, but, within a certain variability, also after randomly directed head-unrestrained gaze shifts to any particular target position [Glenn and Vilis, 1992, Tweed et al., 1995]. These previous studies, however, did not consider the influence of the direction of the saccade preceding a gaze position on torsional orientations. Both in the latter studies and in this thesis the observed torsional thickness of the eye - the torsional variability of eye positions about the fitted surface - was bigger than in studies where the head was fixated: [Tweed and Vilis, 1990] for example found the torsional standard deviation of eye orientations to be 1.5 deg during randomly directed eye-only saccades. [Straumann et al., 1995] found surfaces to be thinner (0.86 deg) in a task that involved primarily horizontal eye-in-head saccades. And [DeSouza and Vilis, 1997] reported an average torsional thickness of about 0.60 deg over a variety of head-fixed gaze shift tasks. It has to be considered that the bigger torsional thickness in head unrestrained gaze shifts could be due to the existence of various different torsional constraints depending on saccade directions. Therefore, the "regardless of how [a gaze direction] was reached" property is of particular importance, when testing Donders' law for validity with the head unrestrained.

In this thesis, it is shown for the first time that torsional constraints of eye-head gaze orientations do not differ for unique or random directions of the preceding saccades. Gaze, head and eye orientations between a condition where the laser target stepped to every target position repeatedly from the *same direction* (Star paradigm) and a condition where the laser target stepped to every target position from *different directions* (Diamond paradigm) were compared. No significant differences could be found between the shapes of the second

order surfaces fitted to gaze, head and eye orientations in the two paradigms (see Figure 4.9). Also, the torsional thickness of the surfaces for the three body units did not differ significantly between the two paradigms (see Figure 4.10). Thus, this study for the first time completely demonstrates all implications of Donders' law for head-unrestrained gaze shifts and particularly shows that its torsional constraints apply independently of saccade directions.

Why, then, is the torsional thickness of eye surfaces bigger after head-unrestrained gaze shifts, as compared to head-fixed (eye-only) gaze shifts? According to [Bernstein, 1967] unveiling the constraints implemented to reduce redundant control parameters provides insight into what the brain is trying to optimize. In that case interpretation of torsional constraints should be easiest for a body unit that most closely adheres to them. The presented data consistently showed the smallest torsional thickness of the head with surfaces that had a pronounced negative twist. Thus, the head rotated counterclockwise for gazes to the upper left and lower right and clockwise for looks to the upper right and lower left. As mentioned in the previous section, this pattern is commonly interpreted as the head moving like a Fick gimbal [Glenn and Vilis, 1992, Theeuwen et al., 1993, Radau et al., 1994, Misslisch et al., 1998]. The anatomical configuration of the head-neck system supports this hypothesis because the atlas (vertical rotations) is mounted on the axis (horizontal rotations) in a gimbal-like way [Richmond and Vidal, 1988]. On the other hand, it has been shown that the head displacement surface can change its shape in a task-dependent manner [Tweed and Vilis, 1992, Ceylan et al., 2000], indicating an optimization of motor performance [Crawford et al., 2003].

For the eye-in-head, the interpretation of torsional constraints is more disputed. Early hypotheses by [Helmholtz, 1867] and [Hering, 1868] favored a perceptual cause, since a displacement *plane* (Listing's plane) optimizes radial image flow on the retina. But only with the head fixed is the eye-in-space (gaze) surface equal to that of the eye-in-head and planar. When the head moves, data in this study show a clear twist in the eye-in-space (gaze) surface, whereas the eye-in-head surface remained flat. Therefore, more recent publications suggested that Listing's plane of the eye-in-head enhances energy efficiency by minimizing

the rotational eccentricity of the eye [Hepp, 1990]. Considering this a change of orientation of Listing's plane would be expected with head movements to maintain efficiency. This has been shown in different contexts: [Misslisch et al., 1998] showed that the pitch of Listing's plane in the head changes with horizontal head rotation. Also, activation of the otolith organs shifts Listing's plane along the torsional axis during static head and body roll relative to gravity [Crawford and Vilis, 1991], and it changes the plane pitch, when head and body are pitched forward or backward [Haslwanter et al., 1992]. Finally, convergent eye movements rotate Listing's plane temporally in the head and vice versa [Allen and Carter, 1967, Van Rijn and Van den Berg, 1993, Bruno and van den Berg, 1997, Kapoula et al., 1999, Steffen et al., 2000]. This proved to be crucial for stereopsis, since the stereo-matching algorithm relies on ocular coordination to keep its eye-fixed search zones aligned during vergence [Schreiber et al., 2001]. Taken together, these observations suggest that when recording head-unrestrained gaze shifts, not a unique Listing's plane, but rather a superposition of several planes tilted at small angles to each other might be measured. This would explain the reported increase of torsional variability about the fitted eye surface in comparison to head-fixed setups.

At last, the torsional thickness of the gaze surfaces was significantly bigger than that of any head or eye surfaces. If one assumes that the brain directly controls the three-dimensional orientation of gaze (eye-in-space), finding that much torsional variability in the presumably controlled entity is unexpected. This led to the formation of new arguments in the discussion about the neuronal control of combined eye-head gaze shifts that is referred to in the next section.

5.3. Interdependencies of Eye- and Head-Control

Half a century ago Bernstein defined coordination as the problem of reducing the number of parameters to perform a particular movement. He observed that unveiling the constraints implemented in motion control provides insight into *what* the brain is trying to optimize [Bernstein, 1967]. Here, Bernstein's question gets taken a step further and it is asked *how* and *where* the eye and head control is implemented.

To answer these questions a model has to be constructed. With relation to *torsional* control of eye-head saccades, any such model would have to provide three-dimensional output. Interestingly, there seems to be only one model of three-dimensional eye-head coordination during head-free gaze shifts [Tweed, 1997]. Still, a good conception of the evolution of models of eye-head gaze control is provided with the following sequence of two-dimensional models, as composed by [Kardamakis and Moschovakis, 2009]:

Linear Summation Hypothesis: Saccades and the vestibulo-ocular reflex sum linearly, such that head contributions to gaze shifts are subtracted from ocular contributions [Bizzi, 1979].

Gaze Feedback Control: Gaze (eye-in-space) is the controlled variable that is compared to instantaneous gaze orientation to create an internal representation of gaze-error driving the head and the eyes [Laurutis and Robinson, 1986, Guitton et al., 1990].

Independent Eye and Head Control: Independent head- and eye-related circuits with cross talk [Phillips et al., 1995, Freedman, 2001].

Which of these models, if they were three-dimensional, would reflect the data reported in this thesis is discussed in the following. Gaze feedback control was already addressed at the end of the previous section: If gaze (eye-in-space) itself was the variable controlled by the brain, and head and eye were driven by a three-dimensional gaze-error, then torsional (and horizontal/vertical) variability of gaze orientations would get minimized. Since in this thesis torsional thickness of the gaze surfaces was the biggest - instead of the smallest -

among the three body units, the model of gaze feedback control is not in agreement with the reported data.

To distinguish between the linear summation hypothesis and the independent eye and head control, it is helpful to note that in the linear summation hypothesis the contributions of the head and the eye (in head) are by definition stochastically dependent on each other. With this, a simple check whether head and eye torsion are in-/dependent will decide for one model or the other. The variance of the sum of independent random variables is the sum of their variances. Torsional thickness is already a measure of variability (the standard deviation of torsional residuals about the fitted surface) and by converting it to variances, the sum of torsional variances of the head and the eye did actually not differ significantly from the variance of gaze (results not shown). So this would already decide in favor of the independent eye and head control, but the effect could simply be caused by two independent sources of noise in the motion systems of the head and the eye, that are big enough to interfere with the dependence of torsional variances.

For this reason, a more robust final test of stochastic in-/dependence was performed. Two variables are dependent, if there is a significant correlation between them. Thus, in the last Results section correlations of head and eye torsion, as averaged over individual fixations, were calculated within every subject. Figure 4.11 shows box plots of the correlation coefficients for the seven subjects, separated by paradigm. It can be easily seen, that the individual subjects exhibited all kinds of strategic preferences. In some cases head and eye torsion were positively correlated, in some cases negatively correlated and in four cases there was no significant correlation. However, *between* subjects the correlation coefficients did not significantly differ from zero, neither for the Star, nor for the Diamond paradigm. With that our data support the more recent models of independent eye and head control.

The three-dimensional model of [Tweed, 1997] is also based on the assumption of independent head and eye controllers. Additionally, it can give an orientation of *where* the eye and head control might be implemented. The model assumes, that the superior colliculus (SC) codes a two-dimensional eye-centered gaze command and that all reference frame transformations and mechanisms for three-dimensional head and eye coordination

are implemented downstream from the SC. This model has been confirmed by studies in head-fixed monkeys [van Opstal et al., 1991, Hepp et al., 1993] and in head-unrestrained monkeys [Klier et al., 2003]. Head and eye movements, elicited by unilateral microstimulations in fixed sites of the SC, not only adhered to the same displacement surfaces as observed in normal behavior, but also varied in size and torsion, depending on their initial position prior to the gaze shift [Klier et al., 2003]. Thus, it was concluded that only the two-dimensional (horizontal/vertical) components of gaze are encoded by the SC. [Klier et al., 2003] argue that in consequence three-dimensional Donders' constraints of the head and the eye must be implemented downstream of the SC.

There is an ongoing dispute whether Donders' law is a result of neural control or simply a consequence of the mechanical properties of the oculomotor plant and the head-neck system. Supporters of the latter hypothesis proposed that for the eye mobile connective tissue insertions on the globe act like "pulleys" that influence the direction of action of the extraocular muscles so that their pulling axes change with eye position [Demer et al., 1995, Crawford et al., 1997, Quaia and Optican, 1998]. Although this *active pulley hypothesis* is well supported, torsional constraints have to be under neural control, since for example Donders' law for the eye fails during sleep [Nakayama, 1975] and during the vestibuloocular reflex [Crawford and Vilis, 1991], and the shape of Donders' surface for the head is task dependent [Ceylan et al., 2000].

According to [Klier et al., 2003], possible target structures for the neural implementation of Donders' law are the nucleus reticularis tegmentis ponti (NRTP) that processes signals for all eye movements that obey Listing's law (saccades [Van Opstal et al., 1996], smooth pursuit [Suzuki et al., 1999], and vergence [Gamlin and Clarke, 1995]), the central mesencephalic reticular formation (cMRF) that returns eye position and velocity feedback to the SC [Pathmanathan et al., 2006b, Pathmanathan et al., 2006a] and indirectly innervates neck muscles via the cervical spinal cord [May et al., 1997], and the interstitial nucleus of cajal (INC), that serves as neural integrator of torsional head and eye positions [Klier et al., 2002, Farshadmanesh et al., 2007]. Studies with patients carrying lesions in the above-mentioned structures are needed to further investigate these hypotheses.

5.4. Outlook on Clinical Application

Two recent clinical studies demonstrated three-dimensional head and eye movement analysis in patients with acute (≤ 5 days) unilateral midbrain lesions [Kremmyda et al., 2007, Kremmyda et al., 2011]. Three out of the five patients in [Kremmyda et al., 2011] had lesions of the INC, which is one of the possible target structures for a neural implementation of Donders' law as described in the previous section. All five had lesions of the rostral interstitial nucleus of the medial longitudinal fasciculus (RIMLF), which serves as the vertical-torsional saccade generator [Büttner and Büttner-Ennever, 2006]. As expected by the model concept presented in the last section, torsional thickness for gaze, head and eye was increased in patients as compared to controls, but this failure of Donders' law was only significant for the eye (in head). What did change for all patients, however, was the *shape* of Donders' surface of the three body units. In particular three of the five patients showed an increased contralesional torsional surface curvature with vertical excursions (coefficient a_4 in this thesis) for gaze, head and eye. For the head, the torsional surface curvature with horizontal excursions (coefficient a_6 in this thesis) was increased in contralesional direction for those three patients.

[Farshadmanesh et al., 2007] report comparable increases of the torsional thickness of the displacement surfaces after reversibly inactivating the INC of three monkeys by unilateral injections of muscimol. In their study, the increase was significant for all three body units. They also observed general torsional offsets of gaze, head and eye in clockwise direction for left INC inactivation and in counterclockwise direction for right INC inactivation. As explained in the first section of this chapter, such changes of the a_1 surface fit parameters could not be detected by [Kremmyda et al., 2011] since calibration sets a_1 to zero both for patients and controls. The shapes of Donders' surfaces changed with unilateral INC inactivation as well. Although inspection of the surfaces showed similar parabolic shapes both for human patients and for monkeys after INC inactivations, the coefficient a_4 and a_6 values differed between the two studies.

These differences in torsional curvatures between the studies of [Kremmyda et al., 2011]

and [Farshadmanesh et al., 2007] could be due to the different time spans elapsed since the lesions. Whereas the monkeys were measured 15 and 60 minutes post injection, the lesions of the patients were up to 5 days old. It is known that there are neural mechanisms that will adapt for failures of torsional constraints. [Fesharaki et al., 2008] showed, that some form of Donders' law of the eyes was reestablished after 4 weeks in patients with brainstem or cerebellar lesions.

Another reason for the differences in torsional curvatures between the two studies could be the dependence of the a_4 and a_6 coefficients on the overall torsional orientation of the displacement surface. Therefore, [Kremmyda et al., 2011] introduced another measure to describe the shape of Donders' surface in a more abstract way. They use the eigenvalues of the second order surface equation to determine the two principal curvatures of the surface independent of its torsional orientation. In the healthy controls Donders' surface of the head always had two opposing curvatures, thus resembling a double saddle. Surfaces of the patients, due to the significant changes in torsional curvature, as described by coefficients a_4 and a_6, lost their double saddle form and became rather parabolic.

In this thesis, all the subjects had opposing eigenvalue signs for the head surfaces as well (results not shown). For the eye, two subjects had a more parabolic or even bowl shaped surface in one of the two paradigms (Star or Diamond). This could also be due to the lack of curvature in the rather planar eye surfaces. For gaze, three subjects did not fulfill the double saddle criterion in one of the paradigms.

If the eigenvalue measure could prove its sensitivity and specificity, it would provide for a simple visual diagnostic tool of failures in three-dimensional eye-head gaze control and could mark the progress of neural adaptation after lesions. Such a three-dimensional measure could not only be used in patients with midbrain and cerebellar lesions. Interestingly, also supranuclear disturbances have shown to change torsional gaze constraints. For example, [Medendorp et al., 1999] showed that the shape of Donders' surface for the head is altered in torticollis. And while there have been investigations of two-dimensional eye-head coordination in patients with Parkinsonism (and cerebellar ataxia) [Shimizu et al., 1981], three-dimensional approaches especially to syndromes with obligatory disturbances of eye

and head control such as progressive supranuclear palsy [Steele et al., 1964] or Cogan's oculomotor apraxia [Cogan, 1953] are lacking.

In conclusion, in the face of such nascent applications of three-dimensional eye and head movement analysis in clinical research and diagnostics, the set of control data thoroughly presented in this thesis will be a valuable asset.

6. Conclusion

This is the first study to simultaneously quantify torsional constraints of the eye and the head in gaze positions independent of the direction of the preceding saccade. The results of this study present three new concepts. Previous studies in humans [Ceylan et al., 2000] and also in monkeys [Crawford et al., 1999] have described subsets of the coefficients and parameters defining torsional surface constraints in eye-head gaze shifts. The present thesis confirms these studies in general and for the first time provides a complete description of all torsional constraint parameters (surface fit coefficients) for each of the three body segments involved (gaze, head and eye). These parameter sets serve as control data for the further study of patients in clinical applications of eye-head coordination. Secondly, it has been suggested in previous studies [Glenn and Vilis, 1992, Tweed et al., 1995] that after randomly directed eye-head gaze shifts to any particular target position the torsional orientation of each of the three body units is similar within a certain variability. In this thesis it can be confirmed that torsional body unit positions are confined to surfaces, and for the first time it is shown that fit coefficients (defining the surface shape) and torisonal thickness of these surfaces do not differ for unique or random directions of the preceding saccades. This finally proves Donders' law for combined eye-head gaze shifts. Thirdly, analysis of torsional variability about the fitted surfaces yielded a new argument supporting recent models of independent eye and head control [Phillips et al., 1995, Freedman, 2001].

Appendix

A. Quaternions

A.1. A Quick Introduction

The extraocular and neck muscles lack special hierarchies for their rotational axes. Rather at each instant, these muscles apply their torques simultaneously and their vectors of torsional moment can be added component-wise to yield a summed torque vector. The rotation produced by this torque vector can be described by a rotation vector which is a single unique rotation axis from some specified reference position and an angle of rotation around it (the length of the vector) [Westheimer, 1957].

Quaternions are composed of a vector part q very similar to a rotation vector and an additional scalar part q_0. They were used in this thesis because, unlike rotation vectors, they provide an accurate and convenient way to perform the non-commutative algebra of three-dimensional rotations (see Appendix section A.2 and [Tweed and Vilis, 1987]). To interpret the data, it is only necessary to understand that q is parallel with the axis of a rotation, and its length is proportional to the magnitude of this rotation. To be specific, a quaternion is related to the axis and magnitude of a rotation as follows:

$$q = n \sin(\alpha/2) \qquad \text{(Equation 0.1)}$$

$$q_0 = \cos(\alpha/2) \qquad \text{(Equation 0.2)}$$

The angle α is the magnitude of the rotation and n is a three-dimensional unit vector parallel to the axis of rotation. The direction of the quaternion vector is determined by the right-hand rule: If the right thumb points in the direction of the quaternion arrow, the fingers of the right hand curl in the direction of the angular displacement from reference position vector to the actual gaze vector. For example at gaze straight ahead α is 0 deg and so $q_0 = 1$ and $q = 0$. The quaternion vector q can be broken down into three components, ordered such that q_1 represents torsional position, q_2 represents vertical position, and q_3 represents horizontal position, with signs arranged to satisfy the right-hand rule.

A.2. Quaternion Mathematics

Recall that quaternions are composed of a scalar component (q_0) and three components (q_1, q_2, q_3) along the standard (right, handed, orthonormal) basis vectors (i, j, k). Quaternions form a four-dimensional vector space. Vectors in three-dimensional space can be regarded

as quaternions with scalar component $q_0 = 0$. If one removes the scalar component of a quaternion q, what is left is called the *vector part* of q.

In addition to the usual vector space operations, there is an operation called *quaternion multiplication* which is defined by the rules:

$$i^2 = j^2 = k^2 = -1$$
$$ij = -ji = k; jk = -kj = i; ki = -ik = j \qquad \text{(Equation 0.3)}$$

Quaternions are added and multiplied like polynomials, keeping the order of the i's, j's and k's aud using the properties in equation Equation 0.3. Then, the quaternion product $r = pq$ can be computed using the formulas:

$$\begin{aligned} r_0 &= p_0q_0 - p_1q_1 - p_2q_2 - p_3q_3 \\ r_1 &= p_0q_1 + p_1q_0 + p_2q_3 - p_3q_2 \\ r_2 &= p_0q_2 + p_2q_0 - p_1q_3 + p_3q_1 \\ r_4 &= p_0q_3 + p_3q_0 + p_1q_2 - p_2q_1 \end{aligned} \qquad \text{(Equation 0.4)}$$

Because i, j and k do not commute, quaternion multiplication, though associative is not commutative. These properties it shares with matrix multiplication and rotations.

For each quaternion q, there is an *inverse*, q^{-1}, such that $qq^{-1} = q^{-1}q = 1$. In general:

$$q^{-1} = (q_0 - q_1i - q_2j - q_3k)/|q|^2 \qquad \text{(Equation 0.5)}$$

In particular, for the unit quaternions used throughout this thesis, $q^{-1} = q_0 - q$. The *division* by a quaternion q is achieved by multiplying with the inverse of q, q^{-1}. In addition to representing rotational displacements, quaternions (q) were used to implement coordinate transformations by rotating another quaternion (p) about the axis n and angle α of q, as follows:

$$qpq^{-1} \qquad \text{(Equation 0.6)}$$

where p can also be a vector with zero scalar component.

B. On the (Non)Additivity of Eye and Head Rotations

Since the head and the eyes have different centers of rotation, it is not literally true that rotations of the head and the eye about their own axes, and through the same angle, will result in the same shift in the gaze direction [Harris, 1994]. Figure 1 displays this situation for a horizontal right visual target at distance d. Since the center of rotation of the eye lies in average 8 centimeters before the center of rotation of the head [Harris, 1994], it alway has to turn by a bigger angle Θ_E than the head's angle Θ_H. Dynamically, every rotation of the head does result in some translation of the eyes. This fact renders our assumption that head and eye rotations sum to the gaze rotation technically inaccurate. Nevertheless, the difference between these estimates goes to zero as the target becomes more distant from the head. For the experiment setup in this thesis (see Methods section 3.3) the assumption of additivity is reasonable as can easily be shown by the calculations according to [Hanes and McCollum, 2006]: The difference between the eye-centered and the head-centered estimates of the gaze shift size for a maximal horizontal target step of 56 deg amounts to 1.37 deg. Thus, in the worst case our calculations for the required eye movements are too small by less than 2% and even this level of discrepancy only occurs for the largest gaze shifts.

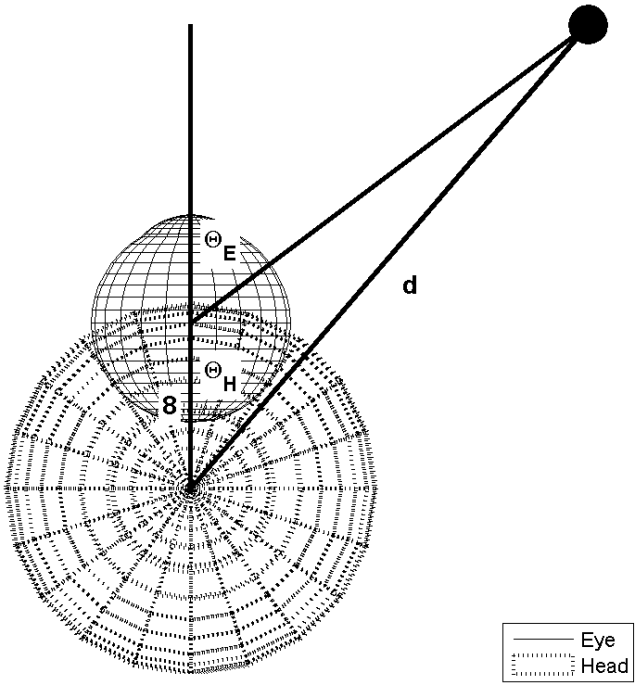

Figure 1.: Angular position of a target with respect to the eye Θ_E and the head Θ_H rotation axes. One can see that Θ_E is always greater than Θ_H, with the difference inversely related to the linear distance d of the target from the head. (Adapted from [Hanes and McCollum, 2006])

C. Informed Consent Paper

Einwilligungserklärung

Herr/ Frau
Geburtsdatum
Adresse
Telefon

Ich wurde darüber aufgeklärt, dass bei mir **Augen- und Kopfbewegungen** untersucht werden sollen. Bei der Untersuchung soll festgestellt werden, welche Rolle einzelne Gehirnareale bei der Auslösung von bestimmten Augen- und Kopfbewegungen haben. Vor der Untersuchung wird mir nach vorheriger Lokalanästhesie mit Augentropfen eine Messspule in Form einer Kontaktlinse (**Coil**) auf das Auge gesetzt. Während der Untersuchung verfolge ich nach Instruktion einen kleinen Lichtpunkt, mit den Augen oder mit dem Kopf. Die Untersuchung dauert ca. **20 min.**. Ich bin darüber aufgeklärt worden, dass meine persönichen Daten aus Gründen des Datenschutzes anonymisiert werden.

Ich bestätige durch meine Unterschrift, dass ich die Probandenaufklärung verstanden habe. Alle von mir gestellten Fragen wurden beantwortet. Ich habe keine weiteren Fragen.

Das Aufklärungsgespräch vor dieser Untersuchung wurde mit

Herrn/ Frau Dr. geführt.

München, den

Unterschrift des Probanden

Bibliography

[Allen and Carter, 1967] Allen, M. J. and Carter, J. H. (1967). The torsion component of the near reflex. A photographic study of the non-moving eye in unilateral convergence. *American Journal of Optometry & Archives of American Academy of Optometry*, 44(6):343–349.

[Aw et al., 1999] Aw, S. T., Halmagyi, G. M., Black, R. A., Curthoys, I. S., Yavor, R. A., and Todd, M. J. (1999). Head impulses reveal loss of individual semicircular canal function. *Journal of Vestibular Research*, 9(3):173–180.

[Bergamin et al., 2004] Bergamin, O., Ramat, S., Straumann, D., and Zee, D. S. (2004). Influence of orientation of exiting wire of search coil annulus on torsion after saccades. *Investigative Ophthalmology & Visual Science*, 45:131–137.

[Bergamin et al., 2001] Bergamin, O., Zee, D. S., Roberts, D. C., Landau, K., Lasker, A. G., and Straumann, D. (2001). Three-dimensional Hess screen test with binocular dual search coils in a three-field magnetic system. *Investigative Ophthalmology & Visual Science*, 42(3):660–667.

[Bernstein, 1967] Bernstein, N. A. (1967). *The Coordination and Regulation of Movements*. Pergamon Press, Oxford, New York.

[Bizzi, 1979] Bizzi, E. (1979). Strategies of eye-head coordination. *Progress in Brain Research*, 50:795–803.

[Bizzi et al., 1971] Bizzi, E., Kalil, R. E., and Tagliasco, V. (1971). Eye-head coordination in monkeys: Evidence for centrally patterned organization. *Science*, 173(3995):452–454.

[Bizzi et al., 1991] Bizzi, E., Mussa-Ivaldi, F. A., and Giszter, S. (1991). Computations underlying the execution of movement: A biological perspective. *Science*, 253(5017):287–291.

[Bruno and van den Berg, 1997] Bruno, P. and van den Berg, A. V. (1997). Relative orientation of primary positions of the two eyes. *Vision Research*, 37(7):935–947.

[Buettner et al., 2002] Buettner, U., Buettner-Ennever, J. A., Rambold, H., and Helmchen, C. (2002). The contribution of midbrain circuits in the control of gaze. *Annals of the New York Academy of Sciences*, 956:99–110.

[Büttner and Büttner-Ennever, 2006] Büttner, U. and Büttner-Ennever, J. A. (2006). Present concepts of oculomotor organization. *Progress in Brain Research*, 151:1–42.

[Ceylan et al., 2000] Ceylan, M. Z., Henriques, D. Y. P., Tweed, D. B., and Crawford, J. D. (2000). Task-dependent constraints in motor control: Pinhole goggles make the head move like an eye. *Journal of Neuroscience*, 20(7):2719–2730.

[Cogan, 1953] Cogan, D. G. (1953). A type of congenital ocular motor apraxia presenting jerky head movements. *American Journal of Ophthalmology*, 36(4):433–441.

[Collewijn et al., 1983] Collewijn, H., Martins, A. J., and Steinman, R. M. (1983). Compensatory eye movements during active and passive head movements: Fast adaptation to changes in visual magnification. *The Journal of Physiology*, 340:259–286.

[Collewijn et al., 1975] Collewijn, H., van der Mark, F., and Jansen, T. C. (1975). Precise recording of human eye movements. *Vision Research*, 15(3):447–450.

[Collewijn et al., 1985] Collewijn, H., Van der Steen, J., Ferman, L., and Jansen, T. C. (1985). Human ocular counterroll: Assessment of static and dynamic properties from electromagnetic scleral coil recordings. *Experimental Brain Research*, 59(1):185–196.

[Crawford et al., 1999] Crawford, J. D., Ceylan, M. Z., Klier, E. M., and Guitton, D. (1999). Three-dimensional eye-head coordination during gaze saccades in the primate. *Journal of Neurophysiology*, 81:1760–1782.

[Crawford et al., 2003] Crawford, J. D., Martinez-Trujillo, J. C., and Klier, E. M. (2003). Neural control of three-dimensional eye and head movements. *Current Opinion in Neurobiology*, 13(6):655–662.

[Crawford and Vilis, 1991] Crawford, J. D. and Vilis, T. (1991). Axes of eye rotation and Listing's law during rotations of the head. *Journal of Neurophysiology*, 65(3):407–423.

[Crawford and Vilis, 1995] Crawford, J. D. and Vilis, T. (1995). How do motor systems deal with the problems of controlling three-dimensional rotations? *Journal of Motor Behavior*, 27(1):89–99.

[Crawford et al., 1997] Crawford, J. D., Vilis, T., and Guitton, D. (1997). Neural coordinate systems for head-fixed and head-free gaze shifts. In Fetter, M., Haslwanter, T., Misslich, H., and Tweed, D., editors, *Three-Dimensional Kinematics of Eye, Head and Limb Movements*, pages 43–56. Harwood Academic Publishers, Amsterdam.

[Demer et al., 2003] Demer, J. L., Kono, R., and Wright, W. (2003). Magnetic resonance imaging of human extraocular muscles in convergence. *Journal of Neurophysiology*, 89(4):2072–2085.

[Demer et al., 1995] Demer, J. L., Miller, J. M., Poukens, V., Vinters, H. V., and Glasgow, B. J. (1995). Evidence for fibromuscular pulleys of the recti extraocular muscles. *Investigative Ophtalmology & Visual Science*, 36(6):1125–1136.

[DeSouza and Vilis, 1997] DeSouza, J. F. X. and Vilis, T. (1997). The shape of Listing's plane. In Fetter, M., Haslwanter, T., Misslich, H., and Tweed, D., editors, *Three-Dimensional Kinematics of Eye, Head and Limb Movements*, pages 101–106. Harwood Academic Publishers, Amsterdam.

[Ditterich and Eggert, 2001] Ditterich, J. and Eggert, T. (2001). Improving the homogeneity of the magnetic field in the magnetic search coil technique. *IEEE Transactions on Biomedical Engineering*, 48(10):1178–1185.

[Donders, 1848] Donders, F. C. (1848). Beitrag zur Lehre von den Bewegungen des menschlichen Auges. *Holländische Beiträge zu den anatomischen und physiologischen Wissenschaften*, 1:105–145.

[Eggert, 2007] Eggert, T. (2007). Eye movement recordings: Methods. *Developments in Ophthalmology*, 40:15–34.

[Enright, 1980] Enright, J. T. (1980). Ocular translation and cyclotorsion due to changes in fixation distance. *Vision Research*, 20(7):595–601.

[Enright, 1984] Enright, J. T. (1984). Saccadic anomalies: Vergence induces large departures from ball-and-socket behavior. *Vision Research*, 24(4):301–308.

[Euler, 1775] Euler, L. (1775). Formulae generales pro translatione quacunque corporum rigidorum. *Commentarii Academiae Scientiarum Imperialis Petropolitanae*, 20:189–207.

[Farshadmanesh et al., 2007] Farshadmanesh, F., Klier, E. M., Chang, P., Wang, H., and Crawford, J. D. (2007). Three-dimensional eye-head coordination after injection of muscimol into the interstitial nucleus of cajal (INC). *Journal of Neurophysiology*, 97(3):2322–2338.

[Ferman et al., 1987] Ferman, L., Collewijn, H., and Van den Berg, A. V. (1987). A direct test of Listing's law – I. Human ocular torsion measured in static tertiary positions. *Vision Research*, 27(6):929–938.

[Fesharaki et al., 2008] Fesharaki, M., Karagiannis, P., Tweed, D., Sharpe, J. A., and Wong, A. M. F. (2008). Adaptive neural mechanism for Listing's law revealed in patients with skew deviation caused by brainstem or cerebellar lesion. *Investigative Ophthalmology & Visual Science*, 49(1):204–214.

[Fetter and Haslwanter, 1999] Fetter, M. and Haslwanter, T. (1999). 3D eye movements–basics and clinical applications. *Journal of Vestibular Research*, 9(3):181–187.

[Fetter et al., 1994] Fetter, M., Tweed, D., Misslisch, H., and Koenig, E. (1994). Three-dimensional human eye movements are organized differently for the different oculomotor subsystems. *Neuro-Ophthalmology*, 14(3):147–152.

[Fick, 1854] Fick, A. (1854). Die Bewegungen des menschlichen Augapfels. *Zeitschrift für rationelle Medizin*, 4:101–128.

[Freedman, 2001] Freedman, E. G. (2001). Interactions between eye and head control signals can account for movement kinematics. *Biological Cybernetics*, 84(6):453–462.

[Gamlin and Clarke, 1995] Gamlin, P. D. and Clarke, R. J. (1995). Single-unit activity in the primate nucleus reticularis tegmenti pontis related to vergence and ocular accommodation. *Journal of Neurophysiology*, 73(5):2115–2119.

[Glasauer et al., 2003] Glasauer, S., Hoshi, M., Kempermann, U., Eggert, T., and Büttner, U. (2003). Three-dimensional eye position and slow phase velocity in humans with downbeat nystagmus. *Journal of Neurophysiology*, 89:338–354.

[Glenn and Vilis, 1992] Glenn, B. and Vilis, T. (1992). Violations of Listing's law after large eye and head gaze shifts. *Journal of Neurophysiology*, 68(1):309–318.

[Guitton et al., 2003] Guitton, D., Bergeron, A., Choi, W. Y., and Matsuo, S. (2003). On the feedback control of orienting gaze shifts made with eye and head movements. *Progress in Brain Research*, 142:55–68.

[Guitton et al., 1990] Guitton, D., Munoz, D. P., and Galiana, H. L. (1990). Gaze control in the cat: Studies and modeling of the coupling between orienting eye and head movements in different behavioral tasks. *Journal of Neurophysiology*, 64(2):509–531.

[Hanes and McCollum, 2006] Hanes, D. A. and McCollum, G. (2006). Variables contributing to the coordination of rapid eye/head gaze shifts. *Biological Cybernetics*, 94(4):300–324.

[Harris, 1994] Harris, L. R. (1994). Visual motion caused by movements of the eye, head and body. In Smith, A. T. and Snowden, R. J., editors, *Visual Detection of Motion*, pages 397–436. Academic Press Ltd., London.

[Haslwanter et al., 1992] Haslwanter, T., Straumann, D., Hess, B. J., and Henn, V. (1992). Static roll and pitch in the monkey: Shift and rotation of Listing's plane. *Vision Research*, 32(7):1341–1348.

[Helmholtz, 1863] Helmholtz, H. v. (1863). Ueber die normalen Bewegungen des menschlichen Auges. *Graefe's Archive for Clinical and Experimental Ophthalmology*, 9(2):153–214.

[Helmholtz, 1867] Helmholtz, H. v. (1867). *Handbuch der physiologischen Optik*. Voss.

[Henn and Straumann, 1999] Henn, V. and Straumann, D. (1999). Three-dimensional eye movement recording for clinical application. *Journal of Vestibular Research*, 9(3):157–162.

[Hepp, 1990] Hepp, K. (1990). On Listing's law. *Communications on Mathematical Physics*, 132:285 – 292.

[Hepp et al., 1993] Hepp, K., Van Opstal, A. J., Straumann, D., Hess, B. J., and Henn, V. (1993). Monkey superior colliculus represents rapid eye movements in a two-dimensional motor map. *Journal of Neurophysiology*, 69(3):965–979.

[Hering, 1868] Hering, E. (1868). *Die Lehre vom binokularen Sehen*. Engelmann, Leipzig.

[Hess and Angelaki, 1997] Hess, B. J. and Angelaki, D. E. (1997). Kinematic principles of primate rotational vestibulo-ocular reflex. I. Spatial organization of fast phase velocity axes. *Journal of Neurophysiology*, 78(4):2193–2202.

[Irving et al., 2003] Irving, E. L., Zacher, J. E., Allison, R. S., and Callender, M. G. (2003). Effects of scleral search coil wear on visual function. *Investigative Ophthalmology & Visual Science*, 44:1933–1938.

[Judge et al., 1980] Judge, S. J., Richmond, B. J., and Chu, F. C. (1980). Implantation of magnetic search coils for measurement of eye position: An improved method. *Vision Research*, 20(6):535–538.

[Kapoula et al., 1999] Kapoula, Z., Bernotas, M., and Haslwanter, T. (1999). Listing's plane rotation with convergence: Role of disparity, accommodation, and depth perception. *Experimental Brain Research*, 126(2):175–186.

[Kardamakis and Moschovakis, 2009] Kardamakis, A. A. and Moschovakis, A. K. (2009). Optimal control of gaze shifts. *The Journal of Neuroscience*, 29(24):7723–7730.

[Klier et al., 2002] Klier, E., Wang, H., Constantin, A., and Crawford, J. (2002). The primate midbrain possesses a neural integrator for torsional and vertical head posture. *Science*, 295:1314–1317.

[Klier et al., 2001] Klier, E. M., Wang, H., and Crawford, J. D. (2001). The superior colliculus encodes gaze commands in retinal coordinates. *Nature Neuroscience*, 4(6):627–632.

[Klier et al., 2003] Klier, E. M., Wang, H., and Crawford, J. D. (2003). Three-dimensional eye-head coordination is implemented downstream from the superior colliculus. *Journal of Neurophysiology*, 89:2839–2853.

[Kremmyda et al., 2007] Kremmyda, O., Büttner-Ennever, J. A., Büttner, U., and Glasauer, S. (2007). Torsional deviations with voluntary saccades caused by a unilateral midbrain lesion. *Journal of Neurology, Neurosurgery & Psychiatry*, 78(10):1155–1157.

[Kremmyda et al., 2011] Kremmyda, O., Glasauer, S., Guerrasio, L., and Büttner, U. (2011). Effects of unilateral midbrain lesions on gaze (eye and head) movements. *Annals of the New York Academy of Sciences*, 1233:71–77.

[Laurutis and Robinson, 1986] Laurutis, V. P. and Robinson, D. A. (1986). The vestibulo-ocular reflex during human saccadic eye movements. *The Journal of Physiology*, 373:209–233.

[May et al., 1997] May, P., Warren, S., and Chen, B. (1997). Pathways for tectal control of vertical eye and head movements. *27th Annual Meeting of the Society for Neuroscience – Abstracts*, 23:842.

[Medendorp et al., 1998] Medendorp, W. P., Melis, B. J., Gielen, C. C., and Gisbergen, J. A. (1998). Off-centric rotation axes in natural head movements: Implications for vestibular reafference and kinematic redundancy. *Journal of Neurophysiology*, 79(4):2025–2039.

[Medendorp et al., 1999] Medendorp, W. P., van Gisbergen, J. A., Horstink, M. W., and Gielen, C. C. (1999). Donders' law in torticollis. *Journal of Neurophysiology*, 82(5):2833–2838.

[Misslisch et al., 1994] Misslisch, H., Tweed, D., Fetter, M., Sievering, D., and Koenig, E. (1994). Rotational kinematics of the human vestibuloocular reflex. III. Listing's law. *Journal of Neurophysiology*, 72(5):2490–2502.

[Misslisch et al., 1998] Misslisch, H., Tweed, D., and Vilis, T. (1998). Neural constraints on eye motion in human eye-head saccades. *Journal of Neurophysiology*, 79(2):859–869.

[Nagel, 1868] Nagel, A. (1868). Ueber das Vorkommen von wahren Rollungen des Auges um die Gesichtslinie. *Graefe's Archive for Clinical and Experimental Ophthalmology*, 14(2):228–246.

[Nakayama, 1975] Nakayama, K. (1975). Coordination of extraocular muscles. In Lennerstrand, G. and Bach-y-Rita, P., editors, *Basic Mechanisms of Ocular Motility and Their Clinical Implications.*, pages 193–207. Pergamon Press, Oxford, UK.

[Pathmanathan et al., 2006a] Pathmanathan, J. S., Cromer, J. A., Cullen, K. E., and Waitzman, D. M. (2006a). Temporal characteristics of neurons in the central mesencephalic reticular formation of head unrestrained monkeys. *Experimental Brain Research*, 168(4):471–492.

[Pathmanathan et al., 2006b] Pathmanathan, J. S., Presnell, R., Cromer, J. A., Cullen, K. E., and Waitzman, D. M. (2006b). Spatial characteristics of neurons in the central mesencephalic reticular formation (cMRF) of head-unrestrained monkeys. *Experimental Brain Research*, 168(4):455–470.

[Phillips et al., 1995] Phillips, J. O., Ling, L., Fuchs, A. F., Siebold, C., and Plorde, J. J. (1995). Rapid horizontal gaze movement in the monkey. *Journal of Neurophysiology*, 73(4):1632–1652.

[Quaia and Optican, 1998] Quaia, C. and Optican, L. M. (1998). Commutative saccadic generator is sufficient to control a 3-D ocular plant with pulleys. *Journal of Neurophysiology*, 79(6):3197–3215.

[Radau et al., 1994] Radau, P., Tweed, D., and Vilis, T. (1994). Three-dimensional eye, head, and chest orientations after large gaze shifts and the underlying neural strategies. *Journal of Neurophysiology*, 72(6):2840–2852.

[Remmel, 1984] Remmel, R. S. (1984). An inexpensive eye movement monitor using the scleral search coil technique. *IEEE Transactions on Biomedical Engineering*, 31(4):388–390.

[Richmond and Vidal, 1988] Richmond, F. J. R. and Vidal, P. P. (1988). The motor system: joints and muscles of the neck. In Peterson, B. W. and Richmond, F. J., editors, *Control of Head Movement*, pages 1–21. Oxford University Press, New York.

[Robinson, 1963] Robinson, D. A. (1963). A method of measuring eye movement using a scleral search coil in a magnetic field. *IEEE Transactions on Biomedical Engineering*, 10:137–145.

[Salvucci and Goldberg, 2000] Salvucci, D. D. and Goldberg, J. H. (2000). Identifying fixations and saccades in eye-tracking protocols. In *ETRA '00: Proceedings of the 2000 Symposium on Eye Tracking Research & Applications*, pages 71–78, New York, NY, USA. ACM.

[Schreiber et al., 2001] Schreiber, K., Crawford, J. D., Fetter, M., and Tweed, D. (2001). The motor side of depth vision. *Nature*, 410(6830):819–822.

[Shimizu et al., 1981] Shimizu, N., Naito, M., and Yoshida, M. (1981). Eye-head coordination in patients with parkinsonism and cerebellar ataxia. *Journal of Neurology, Neurosurgery & Psychiatry*, 44(6):509–515.

[Steele et al., 1964] Steele, J. C., Richardson, J. C., and Olszewski, J. (1964). Progressive supranuclear palsy. A heterogeneous degeneration involving the brain stem, basal ganglia and cerebellum with vertical gaze and pseudobulbar palsy, nuchal dystonia and dementia. *Archives of Neurology*, 10:333–359.

[Steffen et al., 2000] Steffen, H., Walker, M. F., and Zee, D. S. (2000). Rotation of Listing's plane with convergence: Independence from eye position. *Investigative Ophthalmology & Visual Science*, 41(3):715–721.

[Straumann et al., 1991] Straumann, D., Haslwanter, T., Hepp-Reymond, M. C., and Hepp, K. (1991). Listing's law for eye, head and arm movements and their synergistic control. *Experimental Brain Research*, 86(1):209–215.

[Straumann et al., 1995] Straumann, D., Zee, D. S., Solomon, D., Lasker, A. G., and Roberts, D. C. (1995). Transient torsion during and after saccades. *Vision Research*, 35(23-24):3321–3334.

[Suzuki et al., 1999] Suzuki, D. A., Yamada, T., Hoedema, R., and Yee, R. D. (1999). Smooth-pursuit eye-movement deficits with chemical lesions in macaque nucleus reticularis tegmenti pontis. *Journal of Neurophysiology*, 82(3):1178–1186.

[Theeuwen et al., 1993] Theeuwen, M., Miller, L., and Gielen, C. (1993). Are the orientations of the head and arm related during pointing movements? *Journal of Motor Behavior*, 25(3):242–250.

[Turvey, 1990] Turvey, M. T. (1990). Coordination. *American Psychologist*, 45(8):938–953.

[Tweed, 1997] Tweed, D. (1997). Three-dimensional model of the human eye-head saccadic system. *Journal of Neurophysiology*, 77:654–666.

[Tweed et al., 1990] Tweed, D., Cadera, W., and Vilis, T. (1990). Computing three-dimensional eye position quaternions and eye velocity from search coil signals. *Vision Research*, 30(1):97–110.

[Tweed et al., 1995] Tweed, D., Glenn, B., and Vilis, T. (1995). Eye-head coordination during large gaze shifts. *Journal of Neurophysiology*, 73(2):766–779.

[Tweed et al., 1994] Tweed, D., Misslisch, H., and Fetter, M. (1994). Testing models of the oculomotor velocity-to-position transformation. *Journal of Neurophysiology*, 72(3):1425–1429.

[Tweed and Vilis, 1987] Tweed, D. and Vilis, T. (1987). Implications of rotational kinematics for the oculomotor system in three dimensions. *Journal of Neurophysiology*, 58(4):832–849.

[Tweed and Vilis, 1990] Tweed, D. and Vilis, T. (1990). Geometric relations of eye position and velocity vectors during saccades. *Vision Research*, 30(1):111–127.

[Tweed and Vilis, 1992] Tweed, D. and Vilis, T. (1992). Listing's law for gaze-directing head movements. In Berthoz, A., Graf, W., and Vidal, P. P., editors, *The Head-Neck Sensory-Motor System*, pages 387–391. Oxford University Press, New York.

[van Opstal et al., 1991] van Opstal, A. J., Hepp, K., Hess, B. J., Straumann, D., and Henn, V. (1991). Two- rather than three-dimensional representation of saccades in monkey superior colliculus. *Science*, 252(5010):1313–1315.

[Van Opstal et al., 1996] Van Opstal, J., Hepp, K., Suzuki, Y., and Henn, V. (1996). Role of monkey nucleus reticularis tegmenti pontis in the stabilization of Listing's plane. *The Journal of Neuroscience*, 16(22):7284–7296.

[Van Rijn and Van den Berg, 1993] Van Rijn, L. J. and Van den Berg, A. V. (1993). Binocular eye orientation during fixations: Listing's law extended to include eye vergence. *Vision Research*, 33(5-6):691–708.

[von Noorden and Campos, 2002] von Noorden, G. K. and Campos, E. C. (2002). *Binocular Vision and Ocular Motility: Theory and Management of Strabismus*, chapter Physiology of the Ocular Movements, pages 52–84. Mosby, 6th edition.

[Westheimer, 1957] Westheimer, G. (1957). Kinematics of the eye. *Journal of the Optical Society of America*, 47(10):967–974.

[Wong et al., 2002a] Wong, A. M., Sharpe, J. A., and Tweed, D. (2002a). Adaptive neural mechanism for Listing's law revealed in patients with fourth nerve palsy. *Investigative Ophthalmology & Visual Science*, 43(6):1796–1803.

[Wong et al., 2002b] Wong, A. M., Tweed, D., and Sharpe, J. A. (2002b). Adaptive neural mechanism for Listing's law revealed in patients with sixth nerve palsy. *Investigative Ophthalmology & Visual Science*, 43(1):112–119.

[Wong, 2004] Wong, A. M. F. (2004). Listing's law: Clinical significance and implications for neural control. *Survey of Ophthalmology*, 49(6):563–575.

[World Medical Organization, 2004] World Medical Organization (2004). Declaration of Helsinki, 7th (Tokyo) amendment.

Abstract

Under natural conditions the head and the eye are both free to rotate about three mutually orthogonal axes each (horizontal, vertical and torsional). Theoretically, these six degrees of freedom would allow any two-dimensional direction of the line of sight to be obtained by infinitely many torsional head and eye orientations. Yet, for any one gaze direction our brain chooses specific angles of torsion for the head and the eye. For steady fixation of distant targets with the head fixed and upright this observation is known as Donders' law (1847). It has been shown to hold independently of the direction of the rapid gaze shift (saccade) preceding a fixation. Surprisingly, despite considerable research on head and eye coordination the full implications of Donders' law still have not been analyzed for head-unrestrained gaze shifts. It has merely been studied whether torsional constraints hold, when gaze is returned repeatedly to the targets from single initial positions. The aim of this study was to see whether Donders' law holds after head-unrestrained saccades, independently of the saccade direction. Secondary objectives were to analyze whether the neural controls of the eye and the head are dependent or independent during this task and to collect and present control data for comparison with patient recordings in clinical context. Therefore, seven healthy human subjects made large head-unrestrained gaze shifts to a single set of visual targets during two separate conditions: 1) Repeated saccades to individual target positions from the same direction respectively (Star paradigm). 2) Repeated saccades to every target position from several different directions (Diamond paradigm). Three-dimensional orientations of head and eye were measured simultaneously with the magnetic search coil technique and consecutively plotted in three-dimensional space so that those orientations obeying Donders' law formed a surface. For each of the

three body units the static orientations formed subspaces that resembled surfaces in the shape of twisted double saddles. Surfaces of head orientations had the most pronounced twist, eye in head surfaces were the most planar and surfaces of gaze orientations showed intermediate twist. The standard deviation of torsional residuals of the approximated surfaces (torsional thickness) was bigger for gaze than for the eye and smallest for the head. Head and eye torsion, as averaged over individual fixations, were correlated differently within every subject, but between subjects there was no correlation. In summary, neither surface shapes nor torsional thickness of gaze, head or eye differed between the two conditions (Star/Diamond). With this it is shown for the first time that Donders' law of torsional control holds true for gaze, head and eye orientations independently of the direction of the preceding saccade. The absence of correlation between head and eye torsion can be explained by independent controllers of head and eye movements. This yields a new, further argument supporting recent models of neuronal gaze control that are based on the assumption of independent head and eye controllers. Studies with patients carrying lesions in possible target structures of such neuronal controllers are needed to further investigate these models. Finally, clinically-diagnostic relevance of this study arises from the comparison to results of studies on gaze coordination after midbrain lesions where patients exhibit an altered form of Donders' law.

Zusammenfassung

Unter natürlichen Bedingungen sind Rotationen von Kopf und Auge um jeweils drei voneinander unabhängige Raumachsen (Quer-, Hoch- und Längsachse) möglich. Diese sechs Freiheitsgrade würden beim Blick in jede zweidimensionale Richtung beliebige Drehungen um die Längsachse (Torsion) sowohl des Kopfes als auch des Auges erlauben. Unser Gehirn wählt jedoch in jeder Blickrichtung je einen spezifischen Torsionswinkel für Kopf und Auge. Für die Fixation entfernter Blickziele bei aufrechtem, unbewegtem Kopf wurde diese Tatsache als Donders' Law (1847) bekannt. Das Gesetz gilt unabhängig von der Richtung der der Fixation vorhergehenden raschen Blickbewegung (Sakkade). Überraschenderweise wurde trotz zahlreicher Untersuchungen zur Kopf- und Augenkoordination die vollständige Gültigkeit von Donders' Law bei Blickbewegungen mit bewegtem Kopf noch nicht gezeigt. Es wurde lediglich untersucht, ob die resultierenden Torsionsbeschränkungen weiter gelten, wenn der Blick wiederholt von den selben Ausgangspositionen auf verschiedene Punkte gerichtet wird. Hauptziel dieser Arbeit war zu prüfen, ob Donders' Law nach Sakkaden mit bewegtem Kopf unabhängig von der Sakkadenrichtung gilt. Zudem wurde analysiert, ob Kopf und Auge dabei einer gemeinsamen oder separaten neuronalen Kontrolle unterliegen, und es wurden Kontrolldaten zum Vergleich mit Patientenmessungen im klinischen Kontext gesammelt. Dazu führten sieben gesunde menschliche Probanden Sakkaden mit bewegtem Kopf zwischen einer Anordnung visueller Blickziele unter zwei Versuchsbedingungen durch: 1) Wiederholte Sakkaden auf jedes Ziel aus der jeweils gleichen Richtung (Star Paradigma). 2) Wiederholte Sakkaden auf jedes Ziel aus mehreren verschiedenen Richtungen (Diamond Paradigma). Die dreidimensionalen Kopf- und Augenbewegungen wurden simultan mit der magnetischen Search-Coil-Technik gemessen und zur Analyse

räumlich dargestellt, so dass Positionen, die Donders' Law entsprechen, eine Fläche bilden. Für jede der drei Körpereinheiten lagen die statischen Positionen in Unterräumen, die Flächen in Form verdrehter (getwisteter) Doppelsättel ähnelten. Die Flächen der Kopfpositionen wiesen den deutlichsten Twist auf, die der Auge-im-Kopf Positionen waren nahezu eben und die Flächen der Blickpositionen zeigten einen mittleren Twist. Die Standardabweichung der Torsionsresiduen der genäherten Flächen (Torsionsdicke) war größer für den Blick als für das Auge und am kleinsten für den Kopf. Kopf- und Augentorsion, gemittelt über die Einzelfixationen, waren für jeden einzelnen Probanden unterschiedlich korreliert; über alle Probanden ergab sich jedoch keine signifikante Korrelation. Zusammenfassend unterschieden sich weder Flächenform noch Torsionsdicke von Blick, Kopf oder Auge zwischen den beiden Bedingungen (Star/ Diamond). Damit ist zum ersten Mal gezeigt, dass Donders' Law für Blick-, Kopf- und Augenpositionen unabhängig von der Richtung der vorangegangenen Sakkade gilt. Die fehlende Korrelation der Kopf- und Augentorsion ist auf eine unabhängige Kontrolle von Kopf- und Augenbewegungen zurückzuführen. Dies ist ein neues, weiteres Argument zur Bestätigung aktueller Modelle der neuronalen Kontrolle von Blickbewegungen, die von der Annahme unabhängiger Kopf- und Augencontroller ausgehen. Studien mit Patienten, die Läsionen in möglichen Zielstrukturen für solche neuronalen Controller tragen, sind zur weiteren Untersuchung dieser Modelle nötig. Abschließend ergibt sich klinisch-diagnostische Relevanz der Arbeit aus dem Vergleich mit Studiendaten zur Blickkoordination nach Mittelhirnläsionen, bei denen Patienten eine veränderte Form von Donders' Law aufweisen.

Danksagung

Mein aufrichtiger Dank für die Unterstützung, Förderung und Betreuung meiner vorliegenden Dissertation in Verbindung mit verständnisvoller Geduld gilt meinem Doktorvater, Herrn Professor Dr. Ulrich Büttner. Er hat meine Begeisterung für die Neurologie und die Neurowissenschaften geweckt.

Ebenso gilt mein innigster Dank Herrn Dr. Thomas Eggert. Nicht nur für seine freundliche Bereitschaft mich bei meinen Auswertungen zu betreuen, sondern auch für die sehr bereichernden Jahre in denen ich an seiner Seite vertiefende Einblicke in wissenschaftliches Arbeiten gewinnen konnte.

Danken möchte ich auch der Deutschen Forschungsgemeinschaft, die mich und mein Dissertationsvorhaben durch die Gewährung eines Promotionsstipendiums der Graduiertenförderung in großzügiger Weise gefördert hat.

Stellvertretend möchte ich hier Frau Maj-Catherine Botheroyd für ihre freundschaftliche, lockere und großherzige Art, sowie die Organisation und Koordination von zahlreichen Fortbildungen und sozialen Ereignissen danken.

Herrn Professor Dr. Andreas Straube sei an dieser Stelle ein spezieller Dank für die Bereitstellung des Coil-Labors und der Arbeitsmöglichkeiten ausgesprochen. Sein Antreiben bewahrt mich fortwährend davor, den Blick auf das Wesentliche zu verlieren.

Ich danke Frau Dr. Olympia Kremmyda für die Betreuung bei meinen ersten wissenschaftlichen Gehversuchen, die Einweisung in die Coil-Methode und die große Unterstützung bei den Probandenmessungen.

Zudem danke ich Frau Sigrid Langer für ihr immer offenes Ohr in allen Belangen eines Doktoranden im Neurologischen Forschungshaus.

Diese Arbeit wäre nicht entstanden ohne die Bereitschaft der teilnehmenden Probanden, an wissenschaftlicher Forschung mitzuwirken. Ich bedanke mich dafür, dass sie sich alle der aufwändigen Untersuchung unterzogen haben.

Ein besonderer Dank gilt meiner zauberhaften Elisabeth. Deine Liebe und Dein Zuspruch haben mich alle Schwierigkeiten vergessen lassen.

Nicht zuletzt gebührt mein Dank aber meinen Eltern und meiner Familie, ohne deren Höchstmaß an Verständnis, immerwährender Unterstützung und Förderung ich heute nicht an diesem Punkt angelangt wäre.